NASA TECHNICAL MEMORANDUM

NASA TM-78264

INFRARED SCANNER CONCEPT VERIFICATION TEST REPORT

By F. D. Bachtel
Structures and Propulsion Laboratory

January 1980

NASA

George C. Marshall Space Flight Center
Marshall Space Flight Center, Alabama

(NASA-TM-78264) INFRARED SCANNER CONCEPT VERIFICATION TEST REPORT (NASA) 66 p HC A04/MF A01 CSCL 14B

N80-18367

Unclas
G3/35 47336

TECHNICAL REPORT STANDARD TITLE PAGE

1. REPORT NO.	2. GOVERNMENT ACCESSION NO.	3. RECIPIENT'S CATALOG NO.
NASA TM-78264		

4. TITLE AND SUBTITLE

Infrared Scanner Concept Verification Test Report

5. REPORT DATE

January 1980

6. PERFORMING ORGANIZATION CODE

7. AUTHOR(S)

F. D. Bachtel

8. PERFORMING ORGANIZATION REPORT #

9. PERFORMING ORGANIZATION NAME AND ADDRESS

George C. Marshall Space Flight Center
Marshall Space Flight Center, Alabama 35812

10. WORK UNIT NO.

11. CONTRACT OR GRANT NO.

12. SPONSORING AGENCY NAME AND ADDRESS

National Aeronautics and Space Administration
Washington, D.C. 20546

13. TYPE OF REPORT & PERIOD COVERED

Technical Memorandum

14. SPONSORING AGENCY CODE

15. SUPPLEMENTARY NOTES

Prepared by Structures and Propulsion Laboratory, Science and Engineering

16. ABSTRACT

This document presents the test results from a concept verification test program conducted to assess the use of an Infrared Scanner as a remote temperature sensing device for the Space Shuttle program. The Infrared Scanner would be used during prelaunch operations to determine the surface temperature of the External Tank, which contain the cryogenic propellants for the Shuttle Main Engines. The surface of the External Tank is a Spray On Foam Insulation (SOFI) used to thermally insulate the tank and control boiloff of the cryogenic propellants. Under certain weather conditions ice or frost accumulations are likely on the insulation surface, the temperature of which can be significantly below freezing. The Infrared Scanner would be used to assess possible ice/frost accumulations by mapping the insulation surface temperature to detect freezing areas on the tank. The subject test program was conducted during the Fall of 1979 to determine the feasibility of this concept. A total of 127 tests were performed using a typical 8 to 12 micron Infrared Scanner and simulated External Tank surfaces. Areas of investigation included temperature and geometric resolution limits, atmospheric attenuation effects including conditions with fog and rain, and the problem of surface emissivity variations. It was concluded that the basic concept of using an Infrared Scanner to determine near freezing surface temperatures is feasible. The major problem identified was concerned with Infrared reflections which can result in significant errors if not controlled. Action taken to manage these errors will likely result in design and operational constraints to control the viewing angle and surface emissivity. The contents of this report are intended to aid and guide future implementation of this concept.

17. KEY WORDS	18. DISTRIBUTION STATEMENT
	Unclassified-Unlimited

19. SECURITY CLASSIF. (of this report)	20. SECURITY CLASSIF. (of this page)	21. NO. OF PAGES	22. PRICE
Unclassified	Unclassified	67	NTIS

MSFC - Form 3292 (Rev December 1972)

For sale by National Technical Information Service, Springfield, Virginia 22151

TABLE OF CONTENTS

Page

LIST OF ILLUSTRATIONS

LIST OF TABLES

TECHNICAL MEMORANDUM

INFRARED SCANNER CONCEPT VERIFICATION TEST REPORT

1.0 INTRODUCTION

REPRODUCIBILITY OF THE
ORIGINAL PAGE IS POOR

1.1 Test Objectives

The infrared (IR) scanner concept verification test program was a series of tests conducted to assess a typical IR scanner as a remote temperature sensing device for the External Tank (ET) program. Remote sensing of the ET surface temperature will greatly enhance ice/frost predictions which are required in support of launch operations. The primary objectives of these tests were to: (a) determine the accuracy of a typical instrument under varying environmental conditions and viewing configurations, (b) determine the ability of the instrument to display information in a useful format for the intended use, and (c) compare various models of IR scanners.

1.2 Test Summary

The tests were conducted between 9/28/79 and 10/11/79 at the Marshall Space Flight Center (MSFC) in the east test area. Tests were conducted in an open environment at the Test Cell 300 complex, and in an enclosed environment within the Building 4561 High Bay area. A total of 127 tests were performed by MSFC personnel with on-site support from JSC and KSC personnel.

The primary test instrument was an Inframetrics Model 525 Infrared Scanner on loan from the Inframetrics Corporation for this test program. An additional instrument, an AGA model 780, was assessed briefly during a demonstration by AGA personnel. Test results from the AGA scanner are not contained in this report. All test records and data pertaining to the AGA instrument were retained by JSC.

Testing generally consisted of viewing selected targets under varying conditions to assess the IR scanner's response to known target conditions. Recorded data consisted of video tape recordings, still photographs of IR scanner output and test configurations, and printed thermocouple data. All data as well as the detailed test log are being retained by the Thermal Engineering Branch (EP44).

1.3 Summary of Conclusions

The basic concept of using an IR scanner to determine near-freezing surface temperatures on the ET appears feasible based on the data from this test program. However, some of these data relating to IR reflections must be considered preliminary at this time, due to the small number of observations (data population) as well as uncertainties in the test data. The overall accuracy of the system is estimated to range from ±4.7°F for the worst case to ±2.7°F for the best case, which is considered to be consistent with ice/frost prediction requirements. The major problem anticipated is with IR reflections which can result in significant errors if not controlled. Action taken to manage these errors will probably include viewing angle constraints which will render some of the ET unobservable, and may also require a change in the ET surface coating. Additional testing is recommended to resolve these issues.

2.0 TEST CONFIGURATION

2.1 General

A typical test configuration is depicted in Figure 1 and consisted of: (a) the scanner site where the IR scanner(s) and associated support equipment were located, (b) the target site where the various targets and support equipment were positioned. The scanner equipment and the targets were mobile such that they could be positioned to achieve the desired viewing distance and angles relative to each other and to the Sun, sky, etc. The actual distance, angles, and other configuration information for each test are documented in the detailed test log. Also additional configuration information is provided in the Test Descriptions (Section 3.0).

2.2 Infrared Scanner

The primary test instrument was an Inframetrics Model 525 IR scanner. The vendor's specifications for this instrument are presented in Table 1. The scanner support equipment included power supplies, video tape recorders, and a polaroid camera attachment.

The scanner was operated with either the standard lens or an optional 3 power telescope lens. The standard lens had a field of view of 14° × 18° where as the field of view for the 3X lens was 4.5° × 6°.

Primary data recording was on a Sony half-inch reel-to reel video tape machine. Approximately 6.5 hr of video tape were recorded and are being retained by EP44.

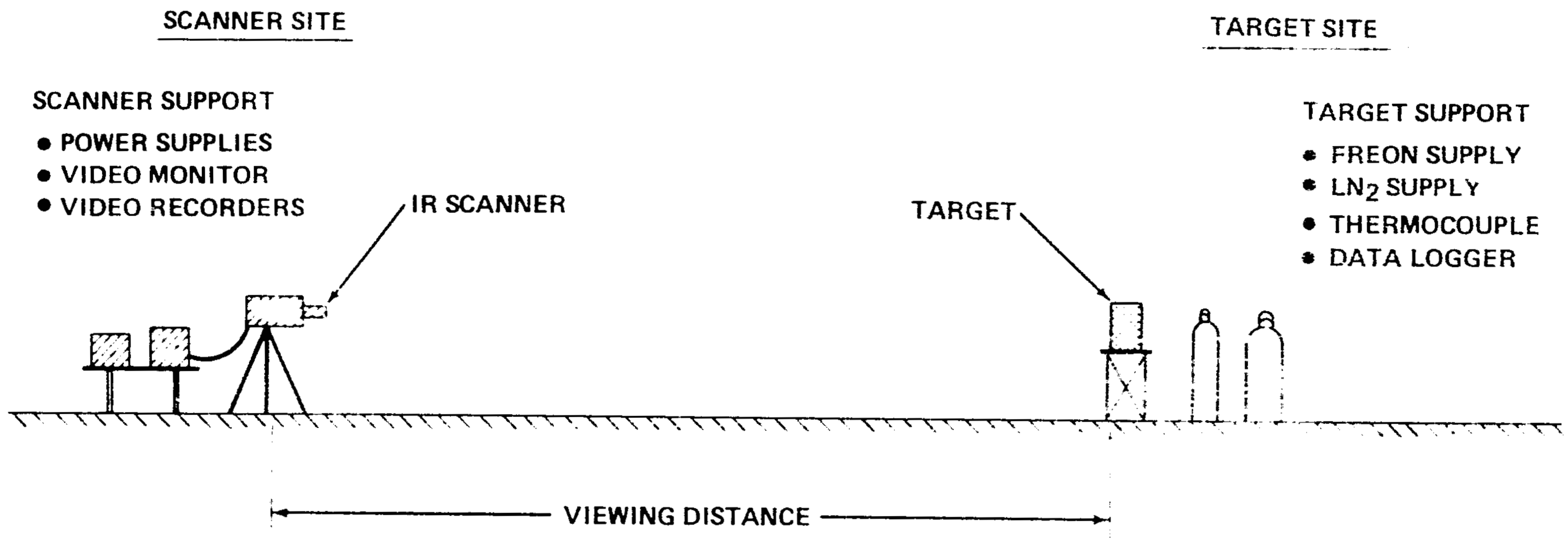

Figure 1. Typical test configuration.

TABLE 1. INFRAMETRICS INFRARED SCANNER SPECIFICATIONS (MODEL 525)

Temperature Measurement Range	-20° to 1500°C
Minimum Detectable Temperature	0.2°C
E O Zoom Range	4:1
Isotherm	10°, 20°, 50°, 100°, 200°, 500° and 1500°C Ranges
Field of View, typical	14° × 18° with 4:1 Zoom
Frame Rate	30 Hz with 2:1 Interlace
Spectral Range	8 to 12 microns
Detector	HgCdTe
Resolvable Elements per Line	>150
Lines Per Frame	525 Raster, >200 IR
Focus Range	5 in. to Infinity
Detector Coolant	Liquid Nitrogen
Coolant Hold Time	>2 hours
Power Requirements	12V Battery or 110 Vac
IR Scanner Size (H×W×L)	5 × 4½ × 6¼ in.
Control/Electronics Unit Size	5½ × 8½ × 8½ in.
IR Scanner Weight	4 lb
Control/Electronics Weight	5½ lb

2.3 Targets

The various targets utilized during the test program included: (a) reference temperature targets which were maintained at known constant temperatures, (b) several masks used in conjunction with the reference targets for resolution tests, (c) an ET surface simulation target which simulated ET surface conditions including ice/frost accumulation, and (d) several surface coating samples to assess various emissivities and surface texture.

The typical reference target is depicted in Figure 2 and consisted of an aluminum tank insulated on five sides. The uninsulated side was the actual target face and was painted flat black and instrumented as shown in the figure. There were a total of five tanks in three sizes as noted. The tanks were filled with either an ice-water mixture to maintain 32°F, or Freon 114 which maintained a temperature of 38.7°F.

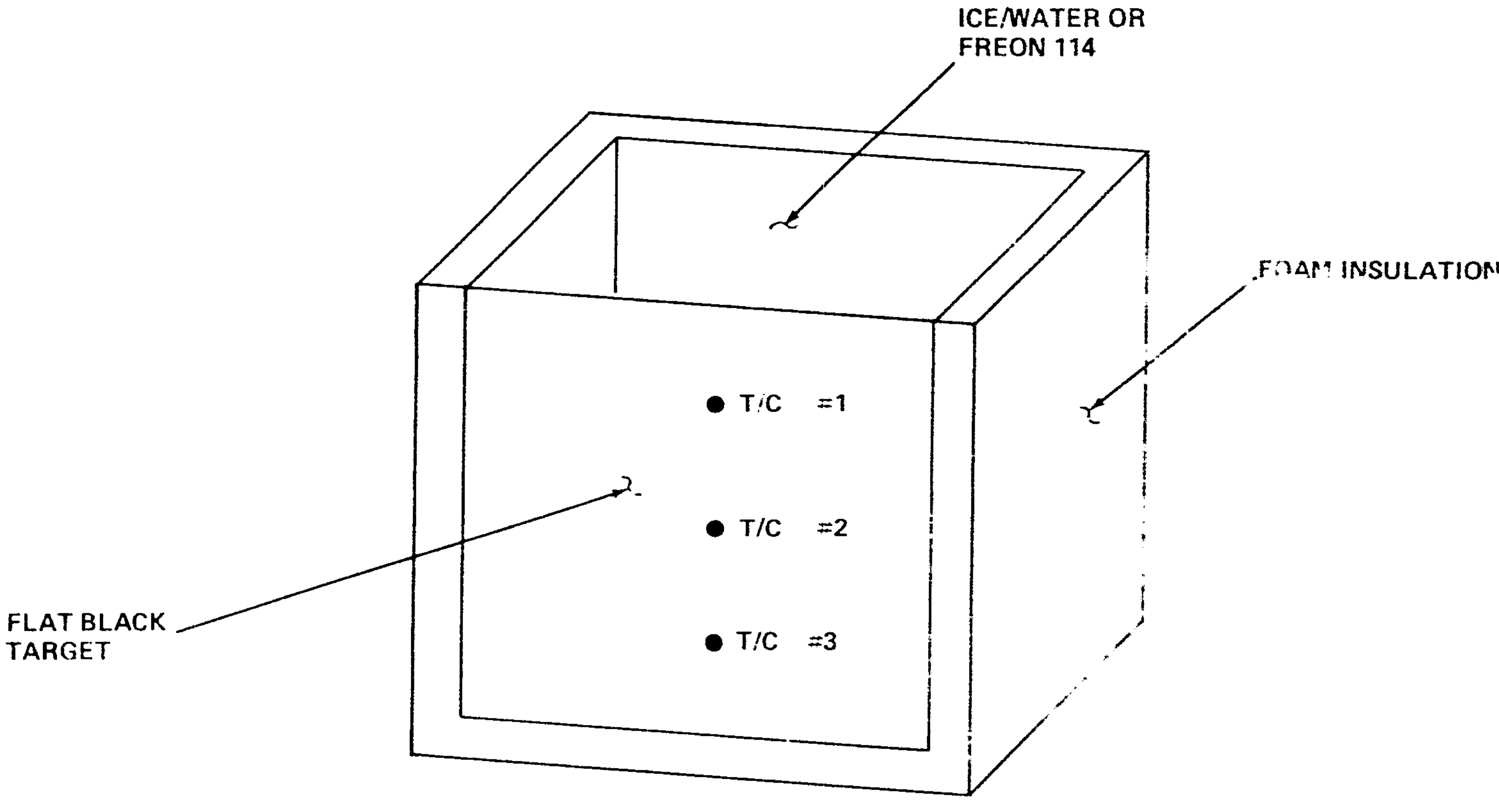

ARTICLE	ABBREVIATIONS	SIZE
SMALL TANKS	S–ICE, S–FRN	12 X 12
LARGE TANKS	L–ICE, L–FRN	30 X 30
ALTERNATE TANK	A–ICE	10 x 10

Figure 2. Reference tank configuration.

The two bar target masks used for geometric resolution tests are depicted in Figure 3. These were constructed from poster board and were positioned directly in front of the large ice reference tank such that the tank could be viewed through the masks. The varying window sizes provided geometric resolution data. An additional mask shown in Figure 4 was used for temperature resolution tests and was mounted on an aluminum horseshoe plate with one leg in ice water and the other in LN_2. The five target windows were instrumented with thermocouples as shown and provided a series of five known temperatures for temperature resolution studies.

The ET surface simulation target is shown in Figure 5 and consists of net spray SOFI applied to an aluminum substrate and mounted to an LN_2 cold plate. The 0.5 in. SOFI thickness enabled icing conditions for the 70°F to 80°F ambient temperatures experienced during the test program. The SOFI surface was instrumented with two thermocouples as shown in the figure.

The various surface coating targets are detailed in Table 2. These targets were used in the IR reflection and Sun reflection tests to assess the effect of surface emissivity and texture, wet and dry, with respect to reflections at various viewing angles. All of the samples were tested at ambient temperature.

TABLE 2. SURFACE COATING TARGETS

Abbreviation	Article	Size (in.)
N-TPS	Net Spray TPS	30 × 30
WN-TPS	Wet Net Spray TPS	30 × 30
W-TPS	White (FRL-3) TPS	30 × 30
WW-TPS	Wet White TPS	30 × 30
B-TPS	Black (flat) TPS	30 × 30
WB-TPS	Wet Black TPS	30 × 30
W-Alum	White Aluminum	30 × 30
WW-Alum	Wet White Aluminum	30 × 30
B-Alum	Black Aluminum	30 × 30
WB-Alum	Wet Black Aluminum	30 × 30
BV-Alum	Black Velvet Aluminum	4 × 4
WBV-Alum	Wet Black Velvet Aluminum	4 × 4

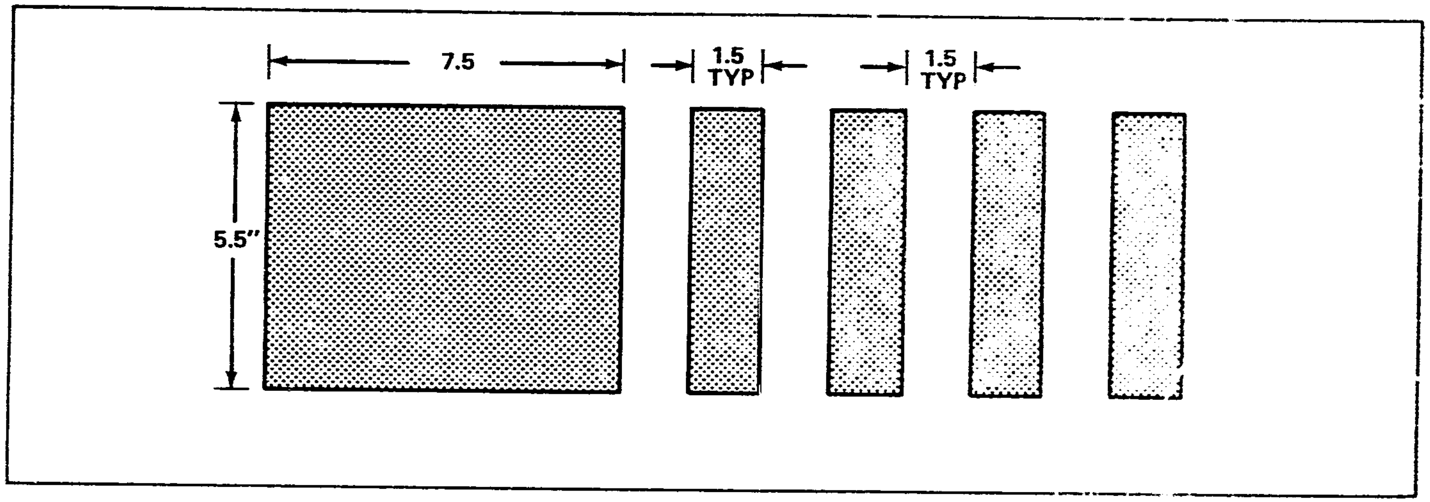

BAR–1

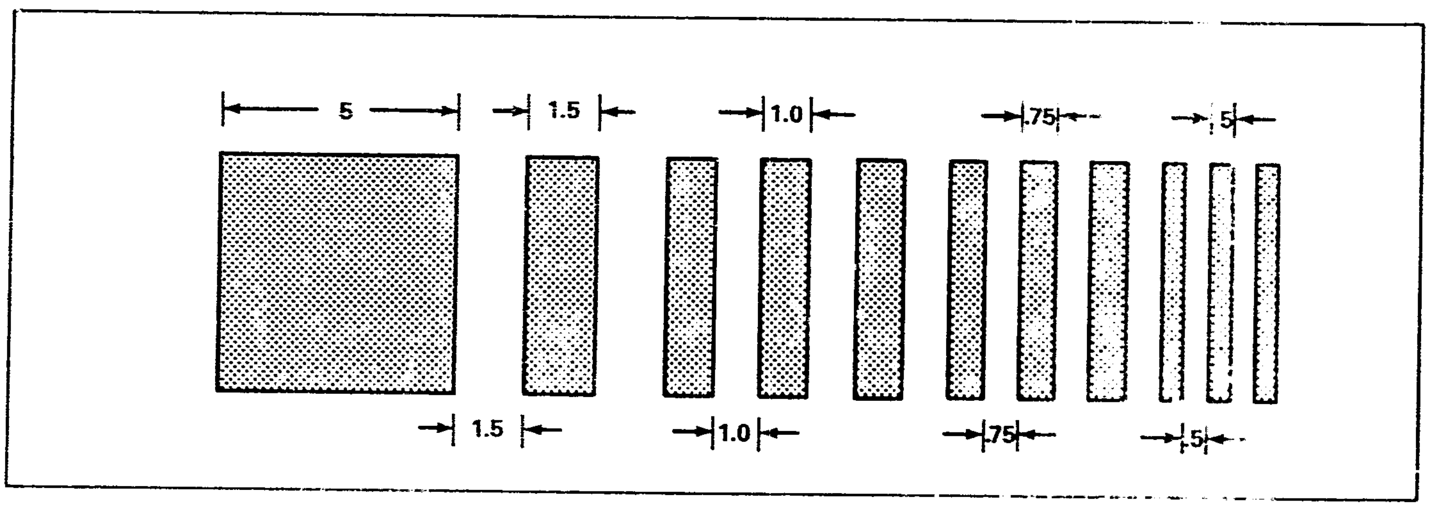

BAR–2

Figure 3. Geometric resolution targets.

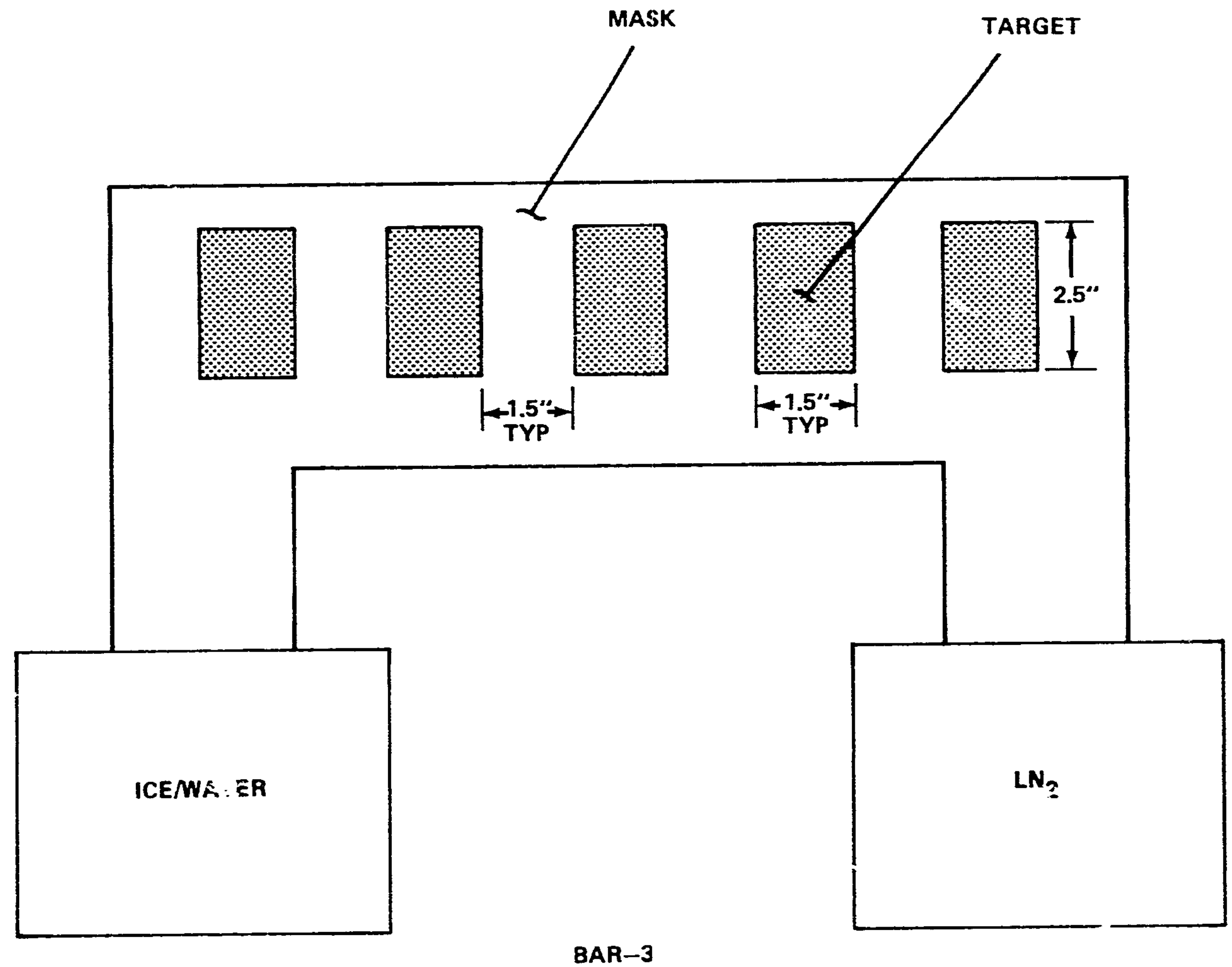

Figure 4. Temperature resolution test article.

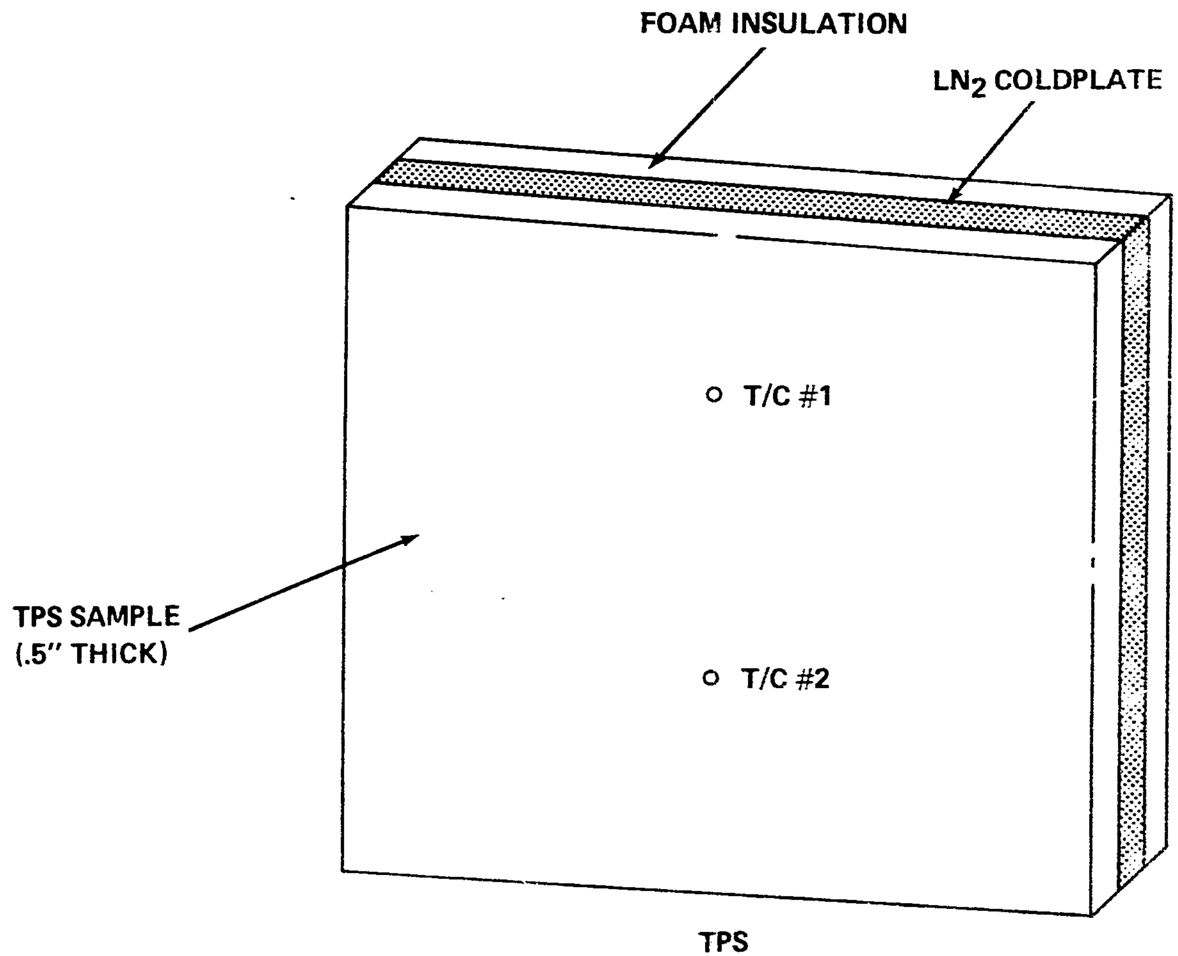

Figure 5. External tank surface simulation target.

3.0 TEST OPERATIONS

3.1 General

A typical test operation consisted of establishing the scanner and target sites in the desired configuration followed by operation of the IR scanner with data being recorded on video tape and in some instances on Polaroid photographs. In addition, still photographs of the scanner site and target site were made for historical documentation and are included in the test log. The reference tanks were checked prior to each test, and refilled and stirred as required to assure proper target face temperatures. The ET surface simulation target was normally operated continuously during a test day, and water was applied to the surface as required to form the desired ice/frost accumulation.

3.2 Infrared Scanner Operation

The Model 525 IR scanner was normally used in each of its three operating modes which include the image mode, the line scan mode, and the isotherm mode. In all modes, data are displayed on a standard TV monitor and for most tests was recorded on video tape. In the image mode, the viewed image is similar to a normal TV picture except the gray scale represents relative temperature differences. Relative temperatures are presented in a continuous range of gray tones from black to white, where the cooler areas can either be choosen dark (normal) or bright (inverted). The image mode provides only qualitative data since the gray scale cannot be visually interpreted quantitatively. To assess actual temperature differences, either the line scan or the isotherm mode was used.

In the line scan mode, a thermal profile is provided in an analog format for any selected horizontal line in the scene. Although the line scan mode can accurately provide a temperature profile, it is limited to the one-dimensional horizontal line currently selected. The isotherm mode provides the same picture as the image mode with the addition that all areas which are at the same selected temperature are highlighted. The temperature to be highlighted is selected using a calibrated marker such that temperature differences within the scene can be determined.

Data obtained from the IR scanner in either the line scan or isotherm modes are raw data in scanner units which must be calibrated to obtain actual temperatures. The calibration or sensitivity must be determined for the current viewing conditions and targets since it is dependent on atmospheric attenuation, target emissivities, and background radiation. In addition, the IR scanner cannot measure absolute temperatures, but only temperature differences. Therefore, a reference target at a known temperature must be viewed to determine absolute temperatures. For most of the tests, an ice-water and Freon reference tank pair were used to determine the sensitivity and the absolute temperature calibration. The line scan and isotherm modes were used throughout the test program to obtain data.

4.0 TEST DESCRIPTIONS

4.1 General

A total of 130 tests were performed during the period from 9/28/79 through 10/11/79, and an abbreviated test log listing each of these tests is presented in Table 3. A test type cross reference which indicates for which tests specific types of data were obtained are included in Table 4. The following sections provide additional detail on these tests and some of the results. Post test analysis of the data is covered in Section 5.0.

4.2 Reference Tests

The reference tests were the first series of tests (1 through 15) and were conducted in the Building 4561 High Bay area. These tests were used to gain familiarization with the IR scanner equipment and to establish the scanner operating characteristics in a controlled environment (i.e., no solar, no cold sky, no wind, etc.). The targets consisted of the small pair of reference tanks and the ET simulation unit. The standard lens and the 3X lens were used, and tests were performed at distances from 25 to 100 ft and at viewing angles from 0° to 70° off normal. It was determined in these tests that the scanner data are independent of the field of view setting (zoom control). This is significant since it allows the operator to zoom in on small targets while maintaining the same sensitivity and calibration obtained with a wider field of view. The sensitivity dropped off slightly at high viewing angles and was apparently caused by an emissivity shift with viewing angle. The sensitivity also dropped off with increasing distance due to atmospheric attenuation. Both these phenomena were investigated further in later tests.

4.3 Fog Tests

A series of eight fog tests was run on the morning of 10/1/79 at Test Cell 300. The visibility was estimated at 500 ft at the beginning of the tests at near 800 ft at the completion. Tests were run at six distances of 75 to 350 ft using the 3X telescope and the pair of small reference tanks. The sensitivity was observed to drop off significantly with distance as was expected; however, the two targets could be easily detected at 350 ft. As was determined later, however, geometric resolution was lost at distances greater than 200 ft (this is independent of fog). The results of these tests are discussed further in Section 5.0.

4.4 Vignetting Tests

These tests (Nos. 26 and 27) were conducted to determine if the optics showed any vignetting effects for the 3X lens and standard lens, respectively. Vignetting effects would be a change in relative

TABLE 3. INFRARED SCANNER VERIFICATION TEST LOG

9/28/79 TESTS INSIDE BLDG 4561 HIGH BAY

1. REFERENCE 1, ICE-TPS-[illegible] AT 25' AT 0 DEG, MAX FOV
2. REFERENCE 2, REPEAT OF TEST 1
3. REFERENCE 3, ICE-TPS-FREON AT 25' AT 30 DEG, MAX FOV
4. REFERENCE 4, ICE-TPS-FREON AT 25' AT 50 DEG, MAX FOV

5. REFERENCE 5, ICE-FREON AT 25' AT 50 DEG, MAX FOV,
6. REFERENCE 6, ICE-FREON AT 25' AT 70 DEG, MAX FOV,
7. REFERENCE 7, ICE-FREON AT 25' AT 70 DEG, FOV SCAN,
8. REFERENCE 8, ICE-FREON AT 25' AT 70 DEG, MIN FOV,
9. REFERENCE 9, REPEAT OF TEST 8
10. REFERENCE 10, ICE-FREON AT 25' AT 50 DEG, MIN FOV,
11. REFERENCE 11, ICE-FREON AT 25' AT 30 DEG, MIN FOV,
12. REFERENCE 12, ICE-FREON AT 25' AT 0 DEG, MIN FOV,
13. REFERENCE 13, ICE-FREON AT 25' AT 0 DEG, FOV SCAN,

14. REFERENCE 14, ICE-TPS-FREON AT 66' AT 0 DEG, MAX FOV, 3X LENS
15. REFERENCE 15, REPEAT OF TEST 14
16. REFERENCE 16, ICE-TPS-FREON AT 100' AT 0 DEG, .75 FOV, 3X LENS
17. REFERENCE 17, ICE-TPS-FREON AT 100' AT 0 DEG, FOV SCAN, 3X LENS

10/1/79 AM TESTS AT CELL 300 IN THE FOG

18. FOG TEST 1, ICE-FREON AT 75' DISTANCE, 3X LENS
19. FOG TEST 2, ICE-FREON AT 100' DISTANCE, 3X LENS
20. FOG TEST 3, ICE-FREON AT 150' DISTANCE, 3X LENS
21. FOG TEST 4, ICE-FREON AT 200' DISTANCE, 3X LENS
22. FOG TEST 5, ICE-FREON AT 250' DISTANCE, 3X LENS
23. FOG TEST 6, ICE-FREON AT 300' DISTANCE, 3X LENS
24. FOG TEST 7, ICE-FREON AT 350' DISTANCE, 3X LENS
25. FOG TEST 8, ICE-FREON AT 75' DISTANCE, 3X LENS

10/2/79 TESTS AT CELL 300 CLEAR AND SUNNY

26. VIGNETTING TEST 1, ICE AT 50' DISTANCE, 3X LENS
27. VIGNETTING TEST 2, ICE AT 25' DISTANCE, STNDRD LENS

28. MULTI-DISTANCE 1, ICE-FREON/ICE AT 25'/25' STNDRD LENS
29. MULTI-DISTANCE 2, ICE-FREON/ICE AT 50'/25' STNDRD LENS
30. MULTI-DISTANCE 3, ICE-FREON/ICE AT 75'/25' STNDRD LENS
31. MULTI-DISTANCE 4, ICE-FREON/ICE AT 100'/25' STNDRD LENS
32. MULTI-DISTANCE 5, ICE-FREON/ICE AT 150'/25' STNDRD LENS
33. MULTI-DISTANCE 6, ICE-FREON/ICE AT 200'/25' STNDRD LENS
34. MULTI-DISTANCE 7, ICE-FREON/ICE AT 25'/25' STNDRD LENS
35. MULTI-DISTANCE 8, ICE-FREON/ICE AT 50'/25' STNDRD LENS

TABLE 3. (Continued)

36. MULTI-DISTANCE 9, ICE-FREON ICE AT 50'/50' 3X LENS
37. MULTI-DISTANCE 10, ICE-FREON/ICE AT 75'/50' 3X LENS
38. MULTI-DISTANCE 11, ICE-FREON/ICE AT 100'/50' 3X LENS
39. MULTI-DISTANCE 12, ICE-FREON/ICE AT 150'/50' 3X LENS
40. MULTI-DISTANCE 13, ICE-FREON/ICE AT 200'/50' 3X LENS
41. MULTI-DISTANCE 14, ICE-FREON/ICE AT 250'/50' 3X LENS
42. MULTI-DISTANCE 14, ICE-FREON/ICE AT 350'/50' 3X LENS
43. MULTI-DISTANCE 15, ICE-FREON/ICE AT 400'/50' 3X LENS
44. MULTI-DISTANCE 16, ICE-FREON/ICE AT 450'/50' 3X LENS
45. MULTI-DISTANCE 17, ICE-FREON/ICE AT 500'/50' 3X LENS

46. VARIABLE DISTANCE 1, ICE AT 3' TO 50', 3X LENS, ISOTHERM MODE
47. VARIABLE DISTANCE 2, ICE AT 3' TO 50', 3X LENS, LINE SCAN MODE

48. SUN REFLECTION 1, SUN ON/OFF ICE-FREON TARGETS (SHUTTERED)
49. SUN REFLECTION 2, SUN ON ICE-FREON AT VARYING TILT ANGLE
50. SUN REFLECTION 3, SUN REFLECTED INTO SCANNER LENS, ICE-FREON VIEWED

10/3/79 TESTS AT CELL 300 CLEAR AND SUNNY

51. SKY BACKGROUND 1, SCAN OF ICE-FREON REF TANKS
52. SKY BACKGROUND 2, SCAN OF ICE-FREON REF TANKS AND SKY

53. TEMP RESOLUTION TEST 1, ICE/ICE
54. TEMP RESOLUTION TEST 2, REPEAT OF TEST 53.
55. TEMP RESOLUTION TEST 3, ICE/ICE WITH LN2 COOLED SURFACE
56. TEMP RESOLUTION TEST 4, ICE/LN2

57. GEOM RESOLUTION 1, ICE/MASK AT 25' DISTANCE, 3X LENS
58. GEOM RESOLUTION 2, ICE/MASK AT 30' DISTANCE, 3X LENS
59. GEOM RESOLUTION 3, ICE/MASK AT 50' DISTANCE, 3X LENS
60. GEOM RESOLUTION 4, ICE/MASK AT 75' DISTANCE, 3X LENS
61. GEOM RESOLUTION 5, ICE/MASK-FREON AT 75' DISTANCE, 3X LENS
62. GEOM RESOLUTION 6, ICE-ICE-FREON 300' DISTANCE, 3X LENS
63. GEOM RESOLUTION 7, ICE-ICE-FREON 200' DISTANCE, 3X LENS
64. GEOM RESOLUTION 8, ICE-ICE-FREON 150' DISTANCE, 3X LENS

65. SUN REFLECTION 4, AMBIENT NET SPRAY SOFI
66. SUN REFLECTION 5, AMBIENT WHITE (FRL-3) SOFI
67. SUN REFLECTION 6, AMBIENT WHITE ALUMINUM
68. SUN REFLECTION 7, AMBIENT NET SPRAY SOFI

69. IR REFLECTION 1, AMBIENT NET SPRAY SOFI
70. IR REFLECTION 2, AMBIENT WHITE (FRL-3) SOFI
71. IR REFLECTION 3, AMBIENT WHITE ALUMINUM
72. IR REFLECTION 4, AMBIENT FLAT BLACK ALUMINUM
73. IR REFLECTION 5, AMBIENT BLACK VELVET ALUMINUM

74. ICE/FROST 1, ICE-TPS-FREON AT 75' DISTANCE

75. LONG DISTANCE 1, ICE-FREON/ICE-FREON AT 800'/75'

TABLE 3. (Continued)

10/4/79 TESTS AT CELL 300 IN RAIN DRIZZLE

76. DRIZZLE VISIBILITY 1, ICE AND FREON TANKS
77. DRIZZLE VISIBILITY 2, ICE TANK ONLY
78. DRIZZLE VISIBILITY 3, GEOM RESOLUTION MASK OVER ICE

79. LONG DISTANCE 2, ICE-FREON/ICE-FREON AT 800'/50' NEAR FOCUS
80. LONG DISTANCE 3, ICE-FREON/ICE-FREON AT 800'/50' FAR FOCUS

81. RADIO INTERFERENCE TEST
82. NO TEST

83. VIDEO TRANSMISSON TEST
    - PART 0 - REFERENCE PATTERN AT TEST SITE
    - PART 1 - AT END OF 800' LINE, NO CONDITIONING
    - PART 2 - AFTER FIRST DISTRIBUTION AMP
    - PART 3 - AFTER APPROX 2 TO 3 MILES DISTRIBUTION
    - PART 4 - REFERENCE PATTERN AT TEST SITE

84. GEOM RESOLUTION 9, ICE/MASK-FREON AT 30' IN DRIZZLE

85. CLOUD OBSERVATION TEST

10/4/79 TEST INSIDE BLDG 4561 HIGH BAY

86. ICE/FROST 2, ICE-FREON-TPS AT 27' WITH 3 MPH FAN
87. ICE/FROST 3, ICE-FREON-TPS AT 75' WITH FLOOD LIGHT
88. ICE/FROST 4, ICE-FREON-TPS AT 75' WITH 10 MPH BLOWER
89. ICE/FROST 5, TPS AT 75' WITH 10 MPH BLOWER
90. ICE/FROST 6, ICE-FREON-TPS AT 75' AT 60 DEG WITH FLOOD AND IR LAMP
91. ICE/FROST 7, TPS AT 75' AT 75 DEG WITH FLOOD AND IR LAMP

92. IR REFLECTION 6, DRY BLACK VELVET AT 20' AT 45 DEG WITH IR LAMP
93. IR REFLECTION 7, WET BLACK VELVET AT 20' AT 45 DEG WITH IR LAMP

94. ICE/FROST 8, ICE-FREON-TPS AT 75' WITH 10 MPH BLOWER

TABLE 3. (Concluded)

10/5/79 TESTS INSIDE BLDG 4561 HIGH BAY

95. GEOM RESOLUTION 9, ICE/MASK1 AT 9'3" DISTANCE, STNDRD LENS
96. GEOM RESOLUTION 10, ICE/MASK2 AT 9'3" DISTANCE, STNDRD LENS

97. IR REFLECTION 8, WET FLAT BLACK ICE TANK AT 17'
98. IR REFLECTION 9, DRY FLAT BLACK ICE TANK AT 17'
99. IR REFLECTION 10, DRY WHITE SOFT AMB PANEL AT 26' REFL OFF LN2 PANEL
100. IR REFLECTION 11, DRY NET SOFT AMB PANEL AT 26' REFL OFF LN2 PANEL
101. IR REFLECTION 12, DRY WHITE ALUM AMB PANEL AT 26' REFL OFF LN2 PANEL
102. IR REFLECTION 13, DRY BLACK ALUM AMB PANEL AT 26' REFL OFF LN2 PANEL
103. IR REFLECTION 14, WET BLACK ALUM AMB PANEL AT 26' REFL OFF LN2 PANEL
104. IR REFLECTION 15, REPEAT OF TEST 103
105. IR REFLECTION 16, DRY WHITE ALUM AMB PANEL AT 26' REFL OFF LN2 PANEL
106. IR REFLECTION 17, WET WHITE ALUM AMB PANEL AT 26' REFL OFF LN2 PANEL
107. IR REFLECTION 18, DRY WHITE SOFT AMB PANEL AT 26' REFL OFF LN2 PANEL
108. IR REFLECTION 19, WET WHITE SOFT AMB PANEL AT 26' REFL OFF LN2 PANEL
109. IR REFLECTION 20, DRY NET SOFT AMB PANEL AT 26' REFL OFF LN2 PANEL
110. IR REFLECTION 21, WET NET SOFT AMB PANEL AT 26' REFL OFF LN2 PANEL
111. IR REFLECTION 22, DRY BLACK VELV AMB PANEL AT 26' REFL OFF LN2 PANEL
112. IR REFLECTION 23, WET BLACK VELV AMB PANEL AT 26' REFL OFF LN2 PANEL
113. IR REFLECTION 24, DRY BLACK VELV AMB PANEL AT 26' REFL OFF LN2 PANEL

10/5/79 TESTS INSIDE BLDG 4561 VIEWING OUTSIDE THRU DOOR

114. SUN REFLECTION 8, DRY NET SOFT AMB PANEL AT 33'
115. SUN REFLECTION 9, DRY WHITE ALUM AMB PANEL AT 33'

10/5/79 TEST INSIDE BLDG 4561 HIGH BAY

116. ICE/FROST 9, TPS AT 65' AT 30 DEG WITH FLOOD LIGHT

10/11/79 TESTS INSIDE BLDG 4561 HIGH BAY

117. IR REFLECTION 25, DRY BLACK ALUM AMB PANEL AT 32' REFL OFF LN2 PANEL
118. IR REFLECTION 26, WET BLACK ALUM AMB PANEL AT 32' REFL OFF LN2 PANEL
119. IR REFLECTION 27, DRY WHITE ALUM AMB PANEL AT 32' REFL OFF LN2 PANEL
120. IR REFLECTION 28, WET WHITE ALUM AMB PANEL AT 32' REFL OFF LN2 PANEL
121. IR REFLECTION 29, DRY BLACK SOFT AMB PANEL AT 32' REFL OFF LN2 PANEL
122. NO TEST
123. IR REFLECTION 30, WET BLACK SOFT AMB PANEL AT 32' REFL OFF LN2 PANEL
124. IR REFLECTION 31, DRY NET SOFT AMB PANEL AT 32' REFL OFF LN2 PANEL
125. NO TEST
126. IR REFLECTION 32, WET NET SOFT AMB PANEL AT 32' REFL OFF LN2 PANEL
127. IR REFLECTION 33, DRY WHITE SOFT AMB PANEL AT 32' REFL OFF LN2 PANEL
128. IR REFLECTION 34, WET WHITE SOFT AMB PANEL AT 32' REFL OFF LN2 PANEL

129. SUN REFLECTION 10, DRY BLACK ALUM AMB PANEL AT 35'
130. SUN REFLECTION 11, DRY WHITE ALUM AMB PANEL AT 35'

TABLE 4. TEST TYPE CROSS REFERENCE

Type	Test Numbers
Reference	1-17
Multi-Distance	28-45, 75, 79, 80
Variable Distance	46, 47
Long Distance	75, 79, 80
Geom Resolution	57-64, 78, 84, 95, 96
Temp Resolution	53-56
Vignetting	26, 27
Sun Reflection	48-50, 65-68, 114, 115, 129, 130
IF Reflection	69-73, 92, 93, 97-113, 117-128
Searchlight Reflection	87, 90, 91
Fog Visibility	18-25
Drizzle Visibility	76-78
Ice/Frost	74, 86-91, 94, 116
Wind	74, 86, 88, 89, 94
Sky Background	51, 52
Radio Interference	81
Video Transmission	83
Cloud Observation	85

temperature (image intensity) as the target of interest is viewed in different portions of the field of view. The small ice reference target was used for these tests, and was positioned in the center and around the perimeter of the field of view. For both tests only minor distortion was experienced and was considered insignificant.

4.5 Multi-Distance Tests

The multiple distance tests were conducted to assess temperature shifts between targets which are viewed at different distances from the scanner. These apparent temperature shifts are due to atmospheric attenuation which cause targets at increasing distances to approach the local ambient temperature. The tests were conducted using the small pair of reference tanks and the alternate ice tank. The alternate ice tank was held at a fixed distance while the pair of ice and Freon tanks were positioned at increasing distances. The near and the far tanks were viewed without adjusting the scanner setpoints such that the apparent temperature shift could be determined.

For tests 28 through 35 the standard lens was used and the fixed target was set at 25 ft and the reference pair positioned at 25 to 200 ft. At distances of 75 ft or more, however, geometric resolution was lost on the reference tank pair. The 3X telescope was used for tests 36 through 45 with the fixed target at 50 ft and the reference pair at 50 to 500 ft. At distances exceeding 200 ft, geometric resolution was lost for this lens. The results of these tests are discussed in detail in Section 5.0.

4.6 Variable Distance Tests

Tests 46 and 47 were similar to the multi distance test except only one ice tank was used. The viewing distance to the tank was varied during the test from 3 to 50 ft by moving the tank with the scanner at a fixed setting. The data from these tests are included with the multi distance tests in Section 5.0.

4.7 Sky Background Tests

These tests were performed with the pair of small reference tanks elevated such that the viewed background was the relatively cold sky rather than the warmer ambient as for most tests. It was somewhat more difficult to acquire the target; however, no significant problems are anticipated with this configuration. It is anticipated that when viewing the ET on the launch pad, much of the tank will be viewed in this manner (e.g., the LOX tank ogive).

4.8 Temperature Resolution Tests

A series of four temperature resolution tests (53 through 56) were performed to assess the basic temperature accuracy of the scanner. The BAR-3 target presented in Figure 4 was used for these tests. The target was conditioned to obtain a range of known temperatures and then viewed with the scanner in the line scan mode along with the small ice reference tank. Data from tests 54, 55, and 56 were processed and are presented in Section 5.0. No data were obtained from test 53.

4.9 Geometric Resolution Tests

Geometric resolution tests were conducted using the BAR-1 and BAR-2 targets presented in Figure 3. These tests were performed at varying distances to determine the percent resolution versus instantaneous field of view. The poster board masks were positioned in front of the large ice tank such that the ice target was viewed through the various size bars cut into the mask. As the targets were moved away from the scanner the percent resolution was noted for the various size bars. The processed data are presented in Section 5.0 and indicate that the actual resolution was somewhat less than vendor specifications. Additional tests were performed under drizzle conditions (78 and 84) and also for the standard lens (95 and 96).

4.10 Sun Reflection Tests

Several tests were run to assess the possibility of interference caused by solar radiation incident either on the target or the scanner. A total of 11 tests were conducted using several surface coatings, both ambient and cold targets, and various Sun angles. The results of these tests did not reveal any interference associated with solar radiation. This is generally to be expected since there is little energy in the portion of the solar spectrum to which the scanner is sensitive.

Test 48 was performed using the small pair of reference tanks positioned in direct sunlight. The Sun was shuttered on and off the targets with no noticeable shift in data. For test 49, the reference tanks were tilted about their horizontal axis to vary the Sun angle. This resulted in significant apparent temperature changes at specific view angles. These temperature shifts however were attributed to emissivity changes with angle, which were observed with and without direct solar.

Test 50 was concerned with solar reflection and possible glare on the scanner lens. Using an aluminum plate as a mirror, the Sun was reflected into the scanner lens at angles as low as 10° from the viewing axis. There was no indication of glare or other interference.

The remaining Sun reflection tests (65 through 68, 114, 115, 129, and 130) were conducted with several of the surface coating targets detailed in Table 2. As before, there was no indication of temperature shifts due to reflected solar energy. The apparent temperature shifts observed in these tests are attributed to background IR reflections since the shifts were observed with or without incident solar energy.

4.11 Infrared Reflection Tests

The purpose of these tests was to assess errors in the measured temperature due to IR reflections. IR reflections occur because most all materials have an emissivity less than unity, and thus have a finite reflectivity in the IR band width of the typical scanner. Thus some of the IR radiation reaching the scanner from a typical target will be reflected energy from the local surroundings (e.g., ground, sky, buildings, etc.). This introduces an error in the sensed temperature since the source of the reflected energy is usually at a different temperature than the target itself. Furthermore, emissivity is known to vary with incident angle for some materials such that a surface tends to become highly reflective at angles approaching 90° off the normal.

The first series of tests (69 through 73) were qualitative tests using the image mode with no actual data being taken. These tests indicated a significant reflection at high off-normal angles for all of the samples, although the black velvet coating seems to be less sensitive than the others. Reflections were noted for rotations about both the horizontal and vertical axis.

Tests 92 and 93 were performed with an IR lamp as a reflection source and the black velvet samples as targets. Test 92 was a dry sample and 93 was a wetted sample. It should be noted that an IR lamp is an extremely high IR radiation source which would not normally be encountered uncontrolled at the launch pad. The dry sample showed very little reflection until angles approaching 60° off-normal. At 80° off normal the reflections were off scale on the scanner (at least 25°F error). The wet sample showed more effect at lower angles being off scale at 45°. In both cases the reflections were more intense at specular angles (angle of incidence of the IR source equal to the viewing angle).

Tests 97 and 98 were conducted with the large ice tank as the target in the Building 4561 High Bay area. In this configuration the local environment (i.e., walls, ceiling, etc.) was the source for the reflections. Since the target (ice) was colder than the ambient, the apparent temperature increased as the target was rotated off normal. Data from this test are presented in Section 5.0.

For tests 97 through 113 and tests 117 through 128, the surface coating samples detailed in Table 2 were used as targets and the LN_2 cold plate surfaces was the reflection source. The test configuration including the position of the scanner, target, and cold plate is shown in Figure 6. In contrast to tests 97 and 98, the apparent temperature decreased as the targets were rotated off normal, since the target and the local ambient were warmer than the reflection source. As with the IR source, the reflection showed a strong specular content with peak reflections occurring when the target-scanner angle and the target-cold plate angle was the same (Fig. 6). Post-test analysis of the data from these tests is also covered in Section 5.0.

4.12 Ice/Frost Tests

The ice/frost tests utilized the ET surface simulation target to assess the scanner performance on targets coated with ice and frost accumulations and to evaluate the data from a target representative of the ET surface, which is non-uniform and thermally dynamic. The ET simulation target (Fig. 5) was conditioned such that ice or frost had formed on approximately 40 percent of the area. The ice ranged from a film to as much as 0.2 in., depending on the test, and frost accumulation occurred generally around the edge of the sample. Test 74 was conducted outside at Cell 300 while the remaining tests (86 through 91, 94, and 116) were conducted inside at the Building 4561 High Bay area.

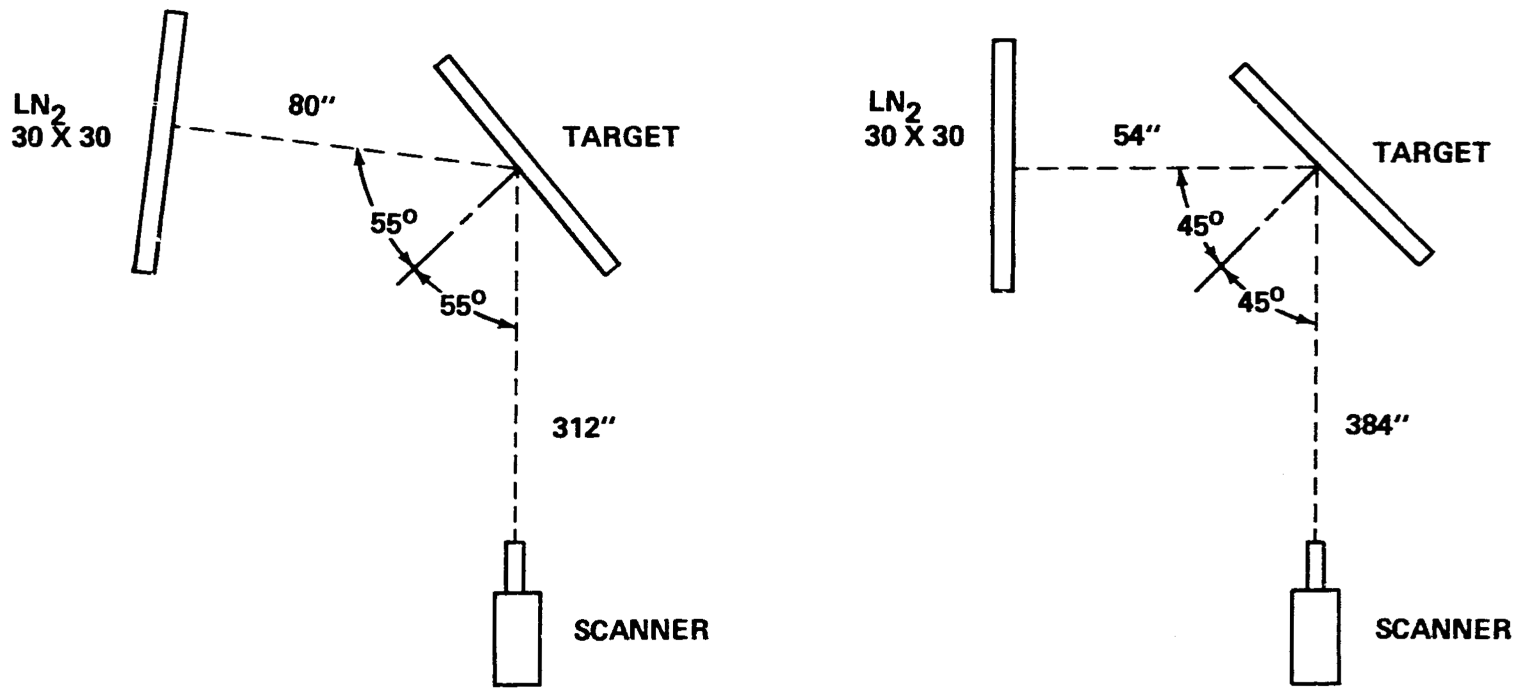

TESTS 99 THRU 113

TESTS 117 THRU 128

Figure 6. IR reflection test configurations.

For test 74, the target was conditioned within a temperature and humidity controlled enclosure prior to the test to promote ice growth. In general, the tests revealed no new anomalies or unexpected results relating to an ice or frost accumulation on the surface. Measured temperatures over the TPS surface ranged from 27°F to approximately 45°F and were consistent with the recorded thermocouple data. There was no distinguishable difference in the image of wet, dry, or ice coated areas other than the temperature difference.

On the outdoor test (74), there were noticeable surface temperature oscillations associated with periodic wind gusts (estimated at 2 to 5 mph), but these were not considered a potential problem. To further investigate wind effects, tests 86, 88, 89, and 94 utilized a portable blower to simulate various wind velocities and cycles (up to 10 mph). As before, the surface temperature could be seen to change rapidly with induced wind cycles. Again, this was not considered a problem since an average surface temperature could be adequately measured.

The remaining ice/frost tests (87, 90, 91, and 116) were concerned with possible reflections from typical search lights which may be used at KSC, and were essentially an extension of the IR reflection tests. Two types of lights were used including a common incandescent flood light and a quartz IR heating lamp. The flood light was typical of sources with little or insignificant energy in the longer IR wavelengths, while the quartz lamp has a high IR energy content. The lamps were positioned approximately 3 to 4 ft from the target at angles ranging from 90° to +90° to the normal. The lamps were oscillated during the test such that reflections could be distinguished from surface temperature changes.

As expected there was minimum reflections encountered with the flood light, and these occurred only at the specular reflection angles. Conversely, the quartz IR lamp caused significant reflections which were strongest at the specular angles. The results of these tests plus the Sun reflection tests previously discussed confirm that the scanner is insensitive to the shorter IR and visible spectrums.

4.13 Long Distance

The long distance tests were an extension of the multi-distance tests designed to assess the scanner performance at relatively long distances. Three tests (75, 79, and 80) were performed with the small pair of reference tanks positioned near the scanner (50 to 75 ft) and the large set of tanks located at 800 ft from the scanner. The test consisted of taking data from the near targets as a baseline and then acquiring the far targets to assess distance effects. The near targets were then reacquired to confirm the original baseline data. Ambient conditions for test 75 was clear and sunny with a low relative humidity of 37 percent. In contrast, tests 79 and 80 were conducted in a light drizzle or mist with an estimated visibility of 1 mile or less. For all the tests, the far target was easily acquired and the sensitivity was great enough to easily distinguish the two targets. The acquired data were in error, however, because the far targets were not geometrically resolved. The resolution for these tests was 85 percent, which is low enough to invalidate the actual data. However, the tests did demonstrate that targets could be acquired at these distances even under adverse conditions. Post-test analysis of data from these tests is presented with the multi distance test data in Section 5.0.

4.14 Drizzle Visibility Tests

A total of nine tests were performed in various degrees of light rain and drizzle at the test Cell 300 complex. Tests 76 through 81 were conducted in the heaviest precipitation with the scanner equipment located in the block house viewing the targets positioned outside. The remaining tests (83 through 85) were conducted in a light suspended mist with all of the equipment outside.

Tests 76, 77, and 78 were at relatively close distance (50 ft) whereas tests 79 and 80 were the long distance tests discussed in the previous section. The only significant effects which may have been caused by the precipitation were observed in tests 76 and 77. During test 76 there was a considerable amount of apparent vapor visible which was degrading the view of the targets. Most of this was attributed to the Freon boiloff, which had been observed on previous tests. For the following test (77), the Freon target was removed and most of the vapor was subsequently eliminated. However, there was still a small amount of vapor periodically visible which could not be attributed to Freon. This vapor did not significantly degrade the image of the target, nor was it observed on any of the other tests under these conditions. Its occurrence however does suggest the possibility of problems associated with precipitation.

4.15 Radio Interference Test

During the test program, two-way radios were periodically used for communications and interference of the scanner operation was commonly observed. Test 81 was specifically conducted to assess radio interference and demonstrated that the scanner was definitely susceptible to RFI. Operation of the radios at close range (within 5 ft) would render the scanner inoperative. Radio frequency shielding for the scanner and/or the support equipment may therefore be required.

4.16 Video Transmission Test

Test 83 was a video transmission test conducted to assess the comp·tibility of the IR scanner with commercial television conditioning and transmission equipment. The scanner was connected to the existing MSFC video network as depicted in Figure 7. There was approximately 750 ft of unconditional line from the scanner site to the first distribution amp in Building 4561. From Building 4561 the amplified signal was routed to Building 4583 where it entered the MSFC wideband distribution system. The signal was then routed to Building 4570 over a cable run of approximately 2.5 miles, where the signal was monitored and recorded. Recordings were also made in Building 4561 before and after the first distribution amplifier. The recordings made at the various points in the distribution system were compared to baseline recordings made at the scanner site to assess any loss of signal or incompatibility with the distribution system. The results were very good with only minor noise being experienced on transmissions of line scan and isotherm data. However, degradation of the gray scale (temperature) information in the image mode could not be assessed with the available equipment.

5.0 TEST ANALYSIS

5.1 Geometric Resolution

A summary of data from the geometric resolution tests is presented in Table 5 which details the field of view and the associated percent resolution for the various target sizes from each test. The field of view (presented in milli-radians) is calculated as FOV = S/D, where S is the bar size and D is the viewing distance in consistent units. The percent resolution was determined from the line scan data recorded for each test and was calculated as $R = Ab/Ao*^{100}$, where Ab was the peak to peak amplitude for the specific bar size and Ao was the reference peak to peak amplitude between ambient and ice.

The percent resolution is plotted versus field of view for the standard lens in Figure 8 and the 3X telescope in Figure 9. For each lens, the assumed modulation transfer function (MTF) curve has been fit to the data and plotted on the appropriate graph. Using the MTF curves from Figure 8, a field of view of at least 16 mrad is required for 100 percent resolution with the standard lens, and from Figure 9, 5.5 mrad is required for complete resolution with the 3X telescope. In both cases, the resolvable element is approximately 5 percent of the total field of view. Using these data, the minimum resolvable target size versus distance was generated for both lens and is presented in Figure 10 for distances up to 300 ft, and in Figure 11 for long distances up to 800 ft. From Figure 10, we see that 100 percent resolution was lost on the small tanks (12 × 12 in.) at 62 ft for the standard lens and 183 ft for the 3X telescope. For purposes of data analysis fror ' ˀ various tests, however, 75 ft was assumed as the cutoff point ˀ ə standard

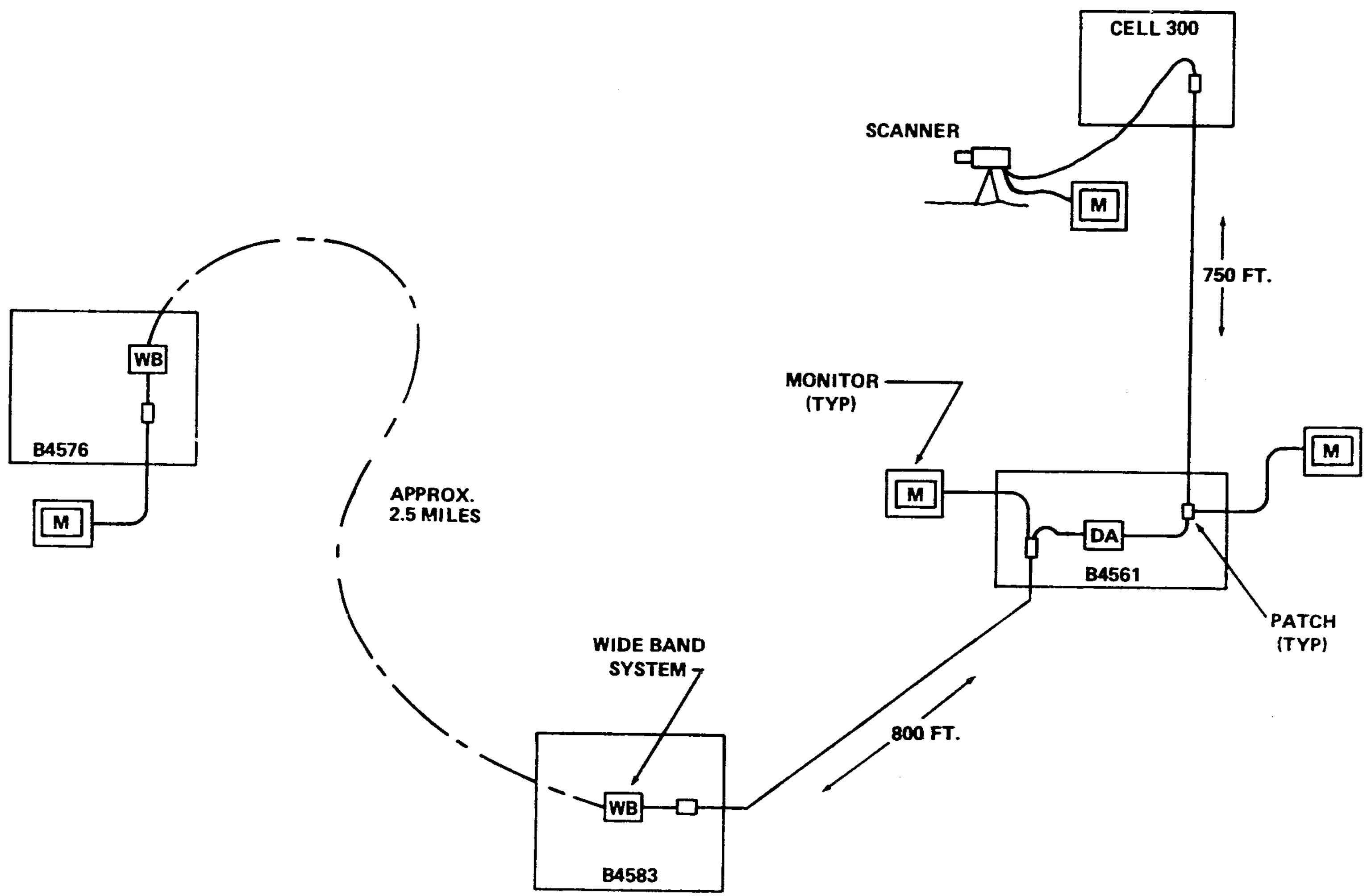

Figure 7. Video transmission test setup.

TABLE 5. TARGET RESOLUTION DATA

TEST	LENS	DIST	TARGET	SIZE	FOV	RES
57	3X	25	BAR 1	1.5	5.0	99%
			BAR 2	1.5	5.0	97%
			BAR 2	1.0	3.33	89%
			BAR 2	.75	2.5	79%
			BAR 2	.50	1.67	68%
58	3X	30.25	BAR 1	1.5	4.13	96%
			BAR 2	1.5	4.13	86%
			BAR 2	1.0	2.75	82%
			BAR 2	.75	2.07	72%
			BAR 2	.50	1.38	64%
59	3X	50	BAR 1	1.5	2.5	83%
			BAR 2	1.5	2.5	80%
			BAR 2	1.0	1.67	62%
			BAR 2	.75	1.25	58%
			BAR 2	.50	.83	36%
60	3X	75	BAR 1	1.5	1.67	70%
			BAR 2	1.5	1.67	72%
			BAR 2	1.0	1.11	60%
			BAR 2	.75	.83	49%
			BAR 2	.50	.56	24%
61	3X	75	BAR 1	1.5	1.67	75%
			BAR 2	1.5	1.67	74%
			BAR 2	1.0	1.11	56%
			BAR 2	.75	.83	49%
			BAR 2	.50	.56	26%
62	3X	300	TANKS	12.0	3.33	93%
63	3X	200	TANKS	12.0	5.0	97%
64	3X	150	TANKS	12.0	6.67	99%
78	3X	50	BAR 1	1.5	2.5	78%
84	3X	30	BAR 2	1.5	4.16	89%
			BAR 2	1.0	2.78	81%
			BAR 2	.75	2.08	70%
			BAR 2	.50	1.39	61%
95	STND	9.25	BAR 1	1.5	13.5	94%
96	STND	9.25	BAR 2	1.5	13.5	94%
			BAR 2	1.0	9.0	81%
			BAR 2	.75	6.76	77%
			BAR 2	.50	4.5	68%

NOTES: Distance (DIST) is in feet
Target size (SIZE) is in inches
Field of view (FOV) is in milli-radians

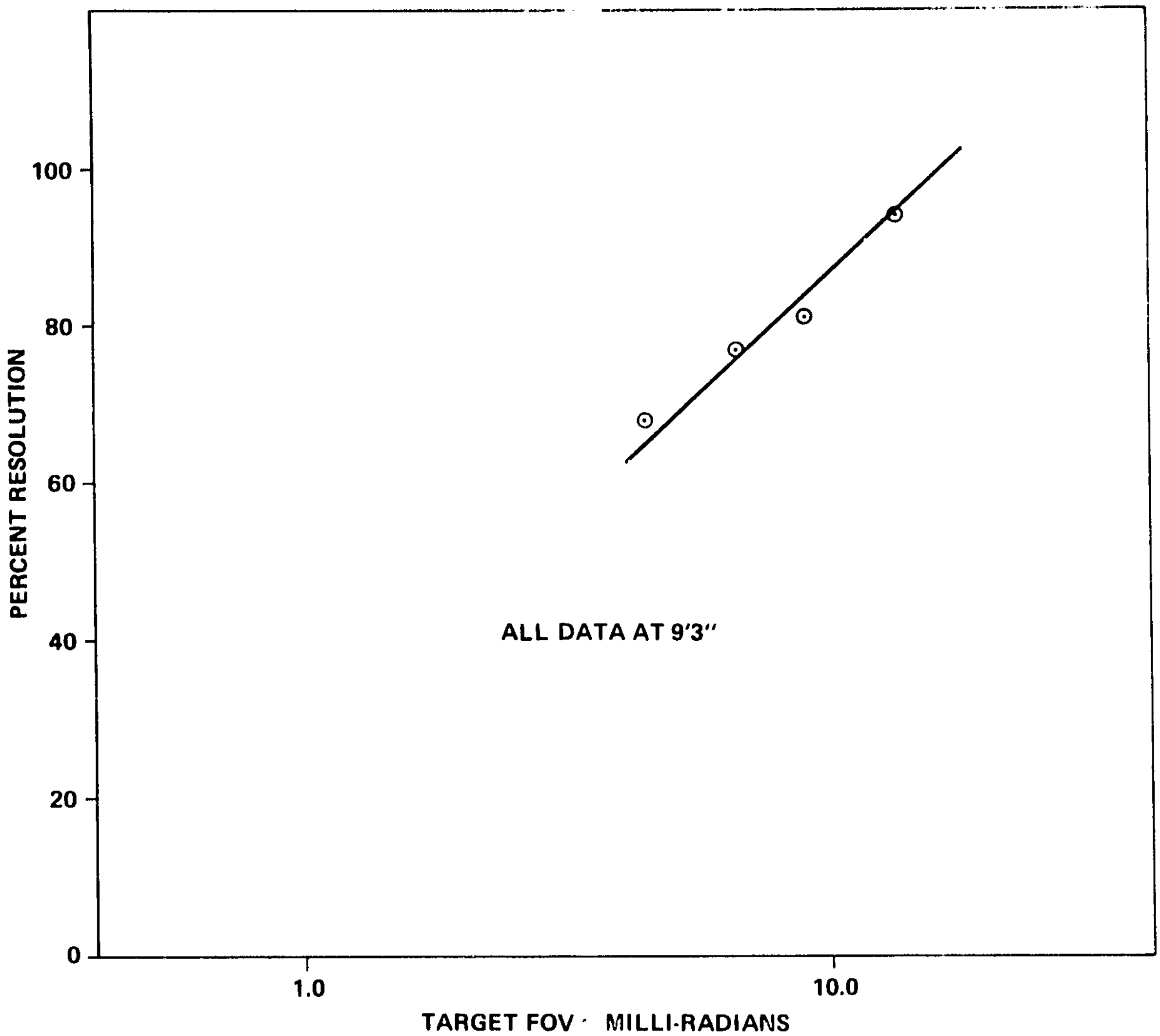

Figure 8. Standard lens resolution data.

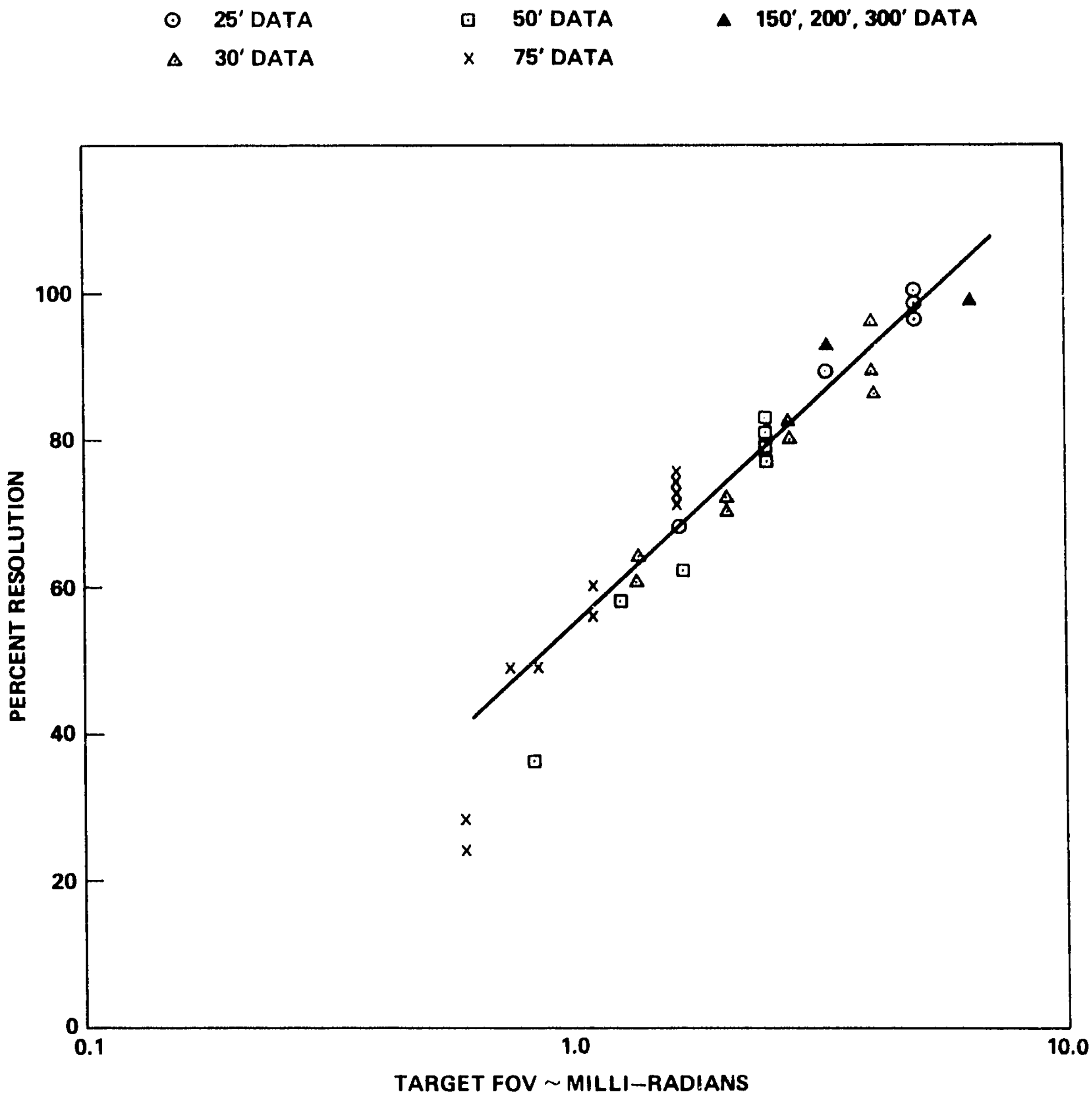

Figure 9. 3X telescope lens resolution data.

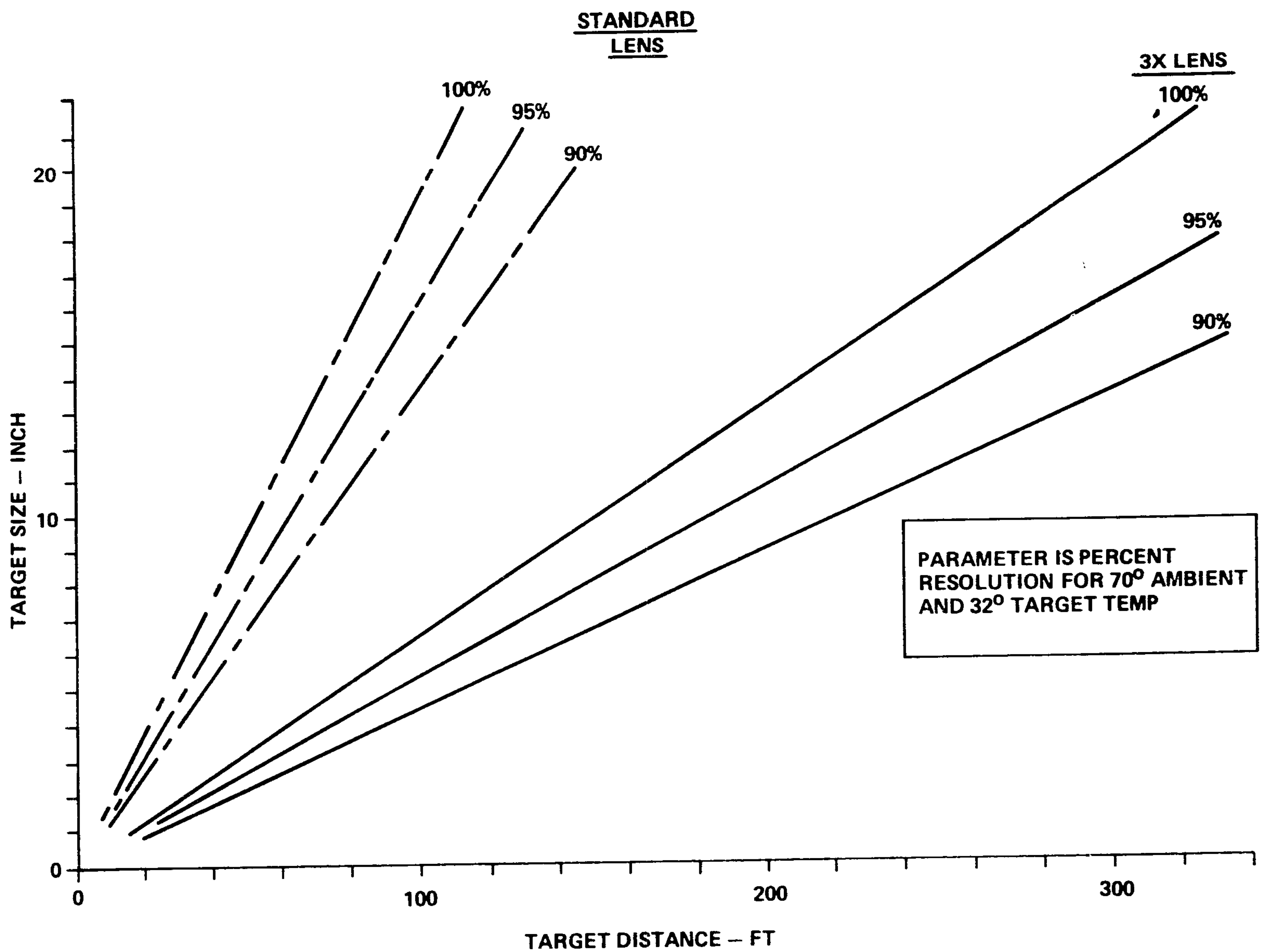

Figure 10. Minimum resoluable target size versus distance.

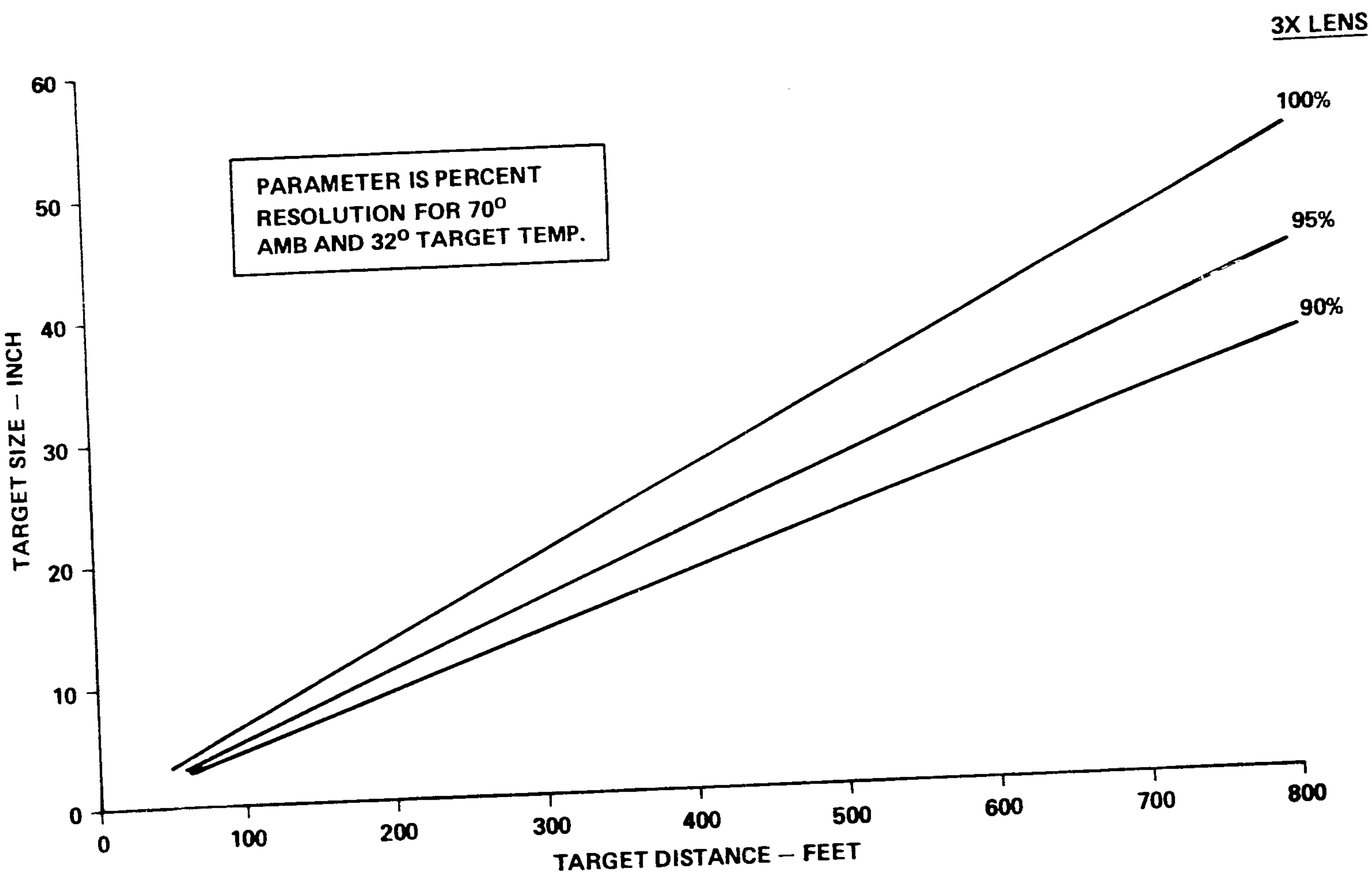

Figure 11. Minimum resoluable target size versus distance (long distance).

lens and 200 ft for the 3X telescope. This relates to a resolution between 95 percent and 100 percent which is considered within the normal error band for the data. Similarly from Figure 11, we see that resolution was lost on the large tanks (30 × 30 in.) at 450 ft for 100 percent resolution and 550 ft for 95 percent resolution.

The apparent temperature error resulting from a typical unresolved target is shown in Table 6 which presents the detail data from test 96. As seen from these data, there is little error experienced for targets which are nearly resolved with only a 0.3°F error on a 94 percent resolved target. However, significant errors are encountered for resolutions below 80 percent with a 3.4°F error on a 77 percent resolved target and a 6.4°F error on a 68 percent resolved target. Consequently, data acquired during this test program on targets which were unresolved must be considered questionable, if not invalid depending on the degree of resolution. Using the data from Figure 8 for the standard lens and Figure 9 for the 3X telescope, the geometric resolution for each of the tests with acquired data was compiled and is presented on Table 7. The field of view (FOV) and the resolution (MTF) is presented for each test in addition to other test information including the lens type, the targets used, and the viewing distance and angle. These data were used in the following analysis to assess the validity of the data involved.

TABLE 6. TYPICAL TEMPERATURE ERROR DUE TO UNRESOLVED TARGETS (DATA TAKEN FROM TEST 96)

Target	Resolution (%)	Measured Level	Calculated Temperature	Temperature Error
Ice	100	.9	32.0*	—
BAR 2.0	100	.9	32.0	0.0
BAR 2.1	94	1.0	32.3	+0.3
BAR 2.2	81	1.4	33.5	+1.5
BAR 2.3	81	1.2	32.9	+0.9
BAR 2.4	81	1.3	33.2	+1.2
BAR 2.5	77	2.0	35.4	+3.4
BAR 2.6	77	2.0	35.4	+3.4
BAR 2.7	77	2.0	35.4	+3.4
BAR 2.8	68	3.0	38.4	+6.4
BAR 2.9	68	3.0	38.4	+6.4
Freon		3.1	38.7*	—

*Note: Assumed Temperatures

In summary, Figures 10 and 11 should be used for determining geometric resolution limits for the standard and 3X telescope lens, respectively. For implementation planning at KSC, resolutions of 95 percent or greater should be maintained. For both lens tested, the resolution was approximately 5 percent of the total field of view.

TABLE 7. TARGET INFORMATION AND RESOLUTION DATA

TEST	TYPE	LENS	TARGETS			DIS	ANG	RSL	FOV	MTF
1	REF	STN	S-ICE	S-FRN	TPS	25	0	R	40	1
2	REF	STN	S-ICE	S-FRN	TPS	25	0	R	40	1
3	REF	STN	S-ICE	S-FRN	TPS	25	30	R	40	1
4	REF	STN	S-ICE	S-FRN	TPS	25	50	R	40	1
5	REF	STN	S-ICE	S-FRN		25	50	R	40	1
6	REF	STN	S-ICE	S-FRN		25	70	R	40	1
7	REF	STN	S-ICE	S-FRN		25	70	R	40	1
8	REF	STN	S-ICE	S-FRN		25	70	R	40	1
9	REF	STN	S-ICE	S-FRN		25	70	R	40	1
10	REF	STN	S-ICE	S-FRN		25	50	R	40	1
11	REF	STN	S-ICE	S-FRN		25	30	R	40	1
12	REF	STN	S-ICE	S-FRN		25	0	R	40	1
13	REF	STN	S-ICE	S-FRN		25	0	R	40	1
14	REF	3X	S-ICE	S-FRN	TPS	66	0	R	15.2	1
15	REF	3X	S-ICE	S-FRN	TPS	66	0	R	15.2	1
16	REF	3X	S-ICE	S-FRN	TPS	100	0	R	10	1
17	REF	3X	S-ICE	S-FRN	TPS	100	0	R	10	1
18	FOG	3X	S-ICE	S-FRN		75	0	R	13.3	1
19	FOG	3X	S-ICE	S-FRN		100	0	R	10	1
20	FOG	3X	S-ICE	S-FRN		150	0	R	6.7	1
21	FOG	3X	S-ICE	S-FRN		200	0	R	5	.98
22	FOG	3X	S-ICE	S-FRN		250	0	U	4	.92
23	FOG	3X	S-ICE	S-FRN		300	0	U	3.3	.87
24	FOG	3X	S-ICE	S-FRN		350	0	U	2.9	.83
25	FOG	3X	S-ICE	S-FRN		75	0	R	13.3	1
26	VIG	3X	S-ICE			50	0	R	20	1
27	VIG	STN	S-ICE			25	0	R	40	1
28	MDIS	STN	S-ICE	S-FRN		25	0	R	40	1
			A-ICE			25	0	R	26.7	1
29	MDIS	STN	S-ICE	S-FRN		50	0	R	20	1
			A-ICE			25	0	R	26.7	1
30	MDIS	STN	S-ICE	S-FRN		75	0	U	13.3	.96
			A-ICE			25	0	R	26.7	1
31	MDIS	STN	S-ICE	S-FRN		100	0	U	10	.88
			A-ICE			25	0	R	26.7	1
32	MDIS	STN	S-ICE	S-FRN		150	0	U	6.7	.77
			A-ICE			25	0	R	26.7	1
33	MDIS	STN	S-ICE	S-FRN		200	0	U	5	.7
			A-ICE			25	0	R	26.7	1
34	MDIS	STN	S-ICE	S-FRN		25	0	R	40	1
			A-ICE			25	0	R	26.7	1
35	MDIS	STN	S-ICE	S-FRN		50	0	R	20	1
			A-ICE			25	0	R	26.7	1
36	MDIS	3X	S-ICE	S-FRN		50	0	R	20	1
			A-ICE			50	0	R	13.3	1
37	MDIS	3X	S-ICE	S-FRN		75	0	R	13.3	1
			A-ICE			50	0	R	13.3	1
38	MDIS	3X	S-ICE	S-FRN		100	0	R	10	1
			A-ICE			50	0	R	13.3	1
39	MDIS	3X	S-ICE	S-FRN		150	0	R	6.7	1
			A-ICE			50	0	R	13.3	1
40	MDIS	3X	S-ICE	S-FRN		200	0	R	5	.98
			A-ICE			50	0	R	13.3	1
41	MDIS	3X	S-ICE	S-FRN		250	0	U	4	.92
			A-ICE			50	0	R	13.3	1

TABLE 7. (Continued)

TEST	TYPE	LENS	T A R G E T S			DIS	ANG	RSL	FOV	MTF
42	MDIS	3X	S-ICE	S-FRN		350	0	U	2.9	.84
			A-ICE			50	0	R	13.3	1
43	MDIS	3X	S-ICE	S-FRN		400	0	U	2.5	.79
			A-ICE			50	0	R	13.3	1
44	MDIS	3X	S-ICE	S-FRN		450	0	U	2.2	.76
			A-ICE			50	0	R	13.3	1
45	MDIS	3X	S-ICE	S-FRN		500	0	U	2	.73
			A-ICE			50	0	R	13.3	1
46	VDIS	3X	S-ICE			50	0	R	20	1
47	VDIS	3X	S-ICE			3	0	R	333.3	1
			S-ICE			50	0	R	20	1
48	SUNR	3X	S-ICE	S-FRN		50	0	R	20	1
49	SUNR	3X	S-ICE	S-FRN		50	0	R	20	1
50	SUNR	3X	S-ICE	S-FRN		100	0	R	10	1
51	SKYB	3X	S-ICE	S-FRN		47	30	R	21.3	1
52	SKYB	3X	S-ICE	S-FRN		47	30	R	21.3	1
53	T-RES	3X	BAR-3			50	0	U	2.5	.79
54	T-RES	3X	BAR-3			50	0	C	2.5	.79
55	T-RES	3X	BAR-3			50	0	C	2.5	.79
56	T-RES	3X	BAR-3			50	0	C	2.5	.79
57	G-RES	3X	BAR-1	BAR-2		25	0	R	16.7	1
58	G-RES	3X	BAR-1	BAR-2		30	0	R	13.9	1
59	G-RES	3X	BAR-1	BAR-2		50	0	R	8.3	1
60	G-RES	3X	BAR-1	BAR-2		75	0	R	5.6	1
61	G-RES	3X	BAR-1	BAR-2	S-FRN	75	0	R	5.6	1
62	G-RES	3X	S-ICE	S-FRN	L-ICE	300	0	U	3.3	.87
63	G-RES	3X	S-ICE	S-FRN	L-ICE	200	0	R	5	.98
64	G-RES	3X	S-ICE	S-FRN	L-ICE	150	0	R	6.7	1
65	SUNR	3X	N-TPS			75	0	R	33.3	1
66	SUNR	3X	W-TPS			75	0	R	33.3	1
67	SUNR	3X	W-ALUM			75	0	R	33.3	1
68	SUNR	3X	N-TPS			75	0	R	33.3	1
69	IRR	3X	N-TPS			75	0	R	33.3	1
70	IRR	3X	W-TPS			75	0	R	33.3	1
71	IRR	3X	W-ALUM			75	0	R	33.3	1
72	IRR	3X	B-ALUM			75	0	R	33.3	1
73	IRR	3X	BV-ALUM			75	0	U	4.4	.95
74	ICE	3X	S-ICE	S-FRN	TPS	75	0	R	13.3	1
75	LDIS	3X	L-ICE	L-FRN		800	0	U	3.1	.85
			S-ICE	S-FRN		75	0	R	13.3	1
76	DRIZ	3X	S-ICE	S-FRN		50	0	R	20	1
77	DRIZ	3X	S-ICE			50	0	R	20	1
78	DRIZ	3X	BAR-2			50	0	R	8.3	1
79	LDIS	3X	L-ICE	L-FRN		800	0	U	3.1	.85
			S-ICE	S-FRN		50	0	R	20	1
80	LDIS	3X	L-ICE	L-FRN		800	0	U	3.1	.85
			S-ICE	S-FRN		50	0	R	20	1
81	RADIO	3X				0	0	R	0	1
82	NOTEST	3X				0	0	R	0	1
83	VIDEO	3X	BAR-2			30	0	R	13.9	1
84	G-RES	3X	BAR-2	S-FRN		30	0	R	13.9	1
85	CLOUD	3X				0	0	R	0	1
86	ICE	3X	S-ICE	S-FRN	TPS	27	0	R	37	1
87	ICE	3X	TPS			75	0	R	33.3	1

TABLE 7. (Concluded)

TEST	TYPE	LENS	TARGETS			DIS	ANG	RSL	FOV	MTF
88	ICE	3X	TPS			75	0	R	33.3	1
89	ICE	3X	TPS			75	0	R	33.3	1
90	ICE	3X	S-ICE	S-FRN	TPS	75	0	R	33.3	1
91	ICE	3X	TPS			75	0	R	33.3	1
92	IRR	3X	BV-ALUM			20	45	R	20.8	1
93	IRR	3X	WBV-ALUM			20	45	R	16.7	1
94	ICE	3X	S-ICE	S-FRN	TPS	75	0	R	33.3	1
95	G-RES	STN	BAR-1			9.25	0	R	45	1
96	G-RES	STN	BAR-2			9.25	0	R	45	1
97	IRR	STN	L-ICE			17	0	R	147.1	1
98	IRR	STN	L-ICE			17	0	R	147.1	1
99	IRR	STN	W-TPS	S-ICE	S-FRN	26	0	R	96.2	1
100	IRR	STN	N-TPS	S-ICE	S-FRN	26	0	R	96.2	1
101	IRR	STN	W-ALUM	S-ICE	S-FRN	26	0	R	96.2	1
102	IRR	STN	B-ALUM	S-ICE	S-FRN	26	0	R	96.2	1
103	IRR	STN	WB-ALUM	S-ICE	S-FRN	26	0	R	96.2	1
104	IRR	STN	WB-ALUM	S-ICE	S-FRN	26	0	R	96.2	1
105	IRR	STN	W-ALUM	S-ICE	S-FRN	26	0	R	96.2	1
106	IRR	STN	WW-ALUM	S-ICE	S-FRN	26	0	R	96.2	1
107	IRR	STN	W-TPS	S-ICE	S-FRN	26	0	R	96.2	1
108	IRR	STN	WW-TPS	S-ICE	S-FRN	26	0	R	96.2	1
109	IRR	STN	N-TPS	S-ICE	S-FRN	26	0	R	96.2	1
110	IRR	STN	WN-TPS	S-ICE	S-FRN	26	0	R	96.2	1
111	IRR	STN	BV-ALUM	S-ICE	S-FRN	26	0	U	12.8	.94
112	IRR	STN	WBV-ALUMS-ICE		S-FRN	26	0	U	12.8	.94
113	IRR	STN	BV-ALUM	S-ICE	S-FRN	26	0	U	12.8	.94
114	SUNR	3X	N-TPS	S-ICE	S-FRN	33	0	R	75.8	1
115	SUNR	3X	W-ALUM	S-ICE	S-FRN	33	0	R	75.8	1
116	ICE	3X	TPS			65	30	R	38.5	1
117	IRR	STN	B-ALUM	S-ICE	S-FRN	32	0	R	78.1	1
118	IRR	STN	WB-ALUM	S-ICE	S-FRN	32	0	R	78.1	1
119	IRR	STN	W-ALUM	S-ICE	S-FRN	32	0	R	78.1	1
120	IRR	STN	WW-ALUM	S-ICE	S-FRN	32	0	R	78.1	1
121	IRR	STN	B-TPS	S-ICE	S-FRN	32	0	R	78.1	1
122	NOTEST	STN				0	0	R	0	1
123	IRR	STN	WB-TPS	S-ICE	S-FRN	32	0	R	78.1	1
124	IRR	STN	N-TPS	S-ICE	S-FRN	32	0	R	78.1	1
125	NOTEST	STN				0	0	R	0	1
126	IRR	STN	WN-TPS	S-ICE	S-FRN	32	0	R	78.1	1
127	IRR	STN	W-TPS	S-ICE	S-FRN	32	0	R	78.1	1
128	IRR	STN	WW-TPS	S-ICE	S-FRN	32	0	R	78.1	1
129	SUNR	50	B-ALUM	S-ICE	S-FRN	0	0	R	0	1
130	SUNR	STN	W-ALUM	S-ICE	S-FRN	50	0	R	50	1

DIS - Target Distance (ft.)
ANG - Angle to Target Normal (Deg.)
RSL - Resolution R = Resolved, U = Unresolved
FOV - Target Field-of-View (milli-radians)
MTF - Modulation Transfer Function (Resolution)

5.2 Temperature Resolution

The temperature resolution tests were performed using the five segment BAR 3 target presented in Figure 4 and discussed in Section 4.8. A total of six data scans were selected from the three tests and the processed data for each is presented in Table 8. The data scans presented were selected to obtain varying temperature profiles ranging from 1.8°F profile on Test 55-0 to a 17°F profile on Test 56-9/10. The data in Table 8 compare the temperature profile as measured by the thermocouples to that determined by the IR scanner. For each test the data from the ice reference and the five target segments are presented and include the scanner level determined from line scan data, the measured thermocouple data, the calculated temperature determined from the scanner level, and the error or difference between the measured (thermocouple) data and the calculated (scanner) data.

Since the Freon reference target was not used in these tests, the scanner sensitivity was determined from the difference between the ice reference and the average of the five segments of the BAR-3 target. The scanner absolute calibration was based on the ice reference, thus the ice target error was always zero.

As shown in Table 8 the maximum temperature error experienced ranged from +1.1°F on test 54-0 to -0.9°F on test 56-9/10 or approximately ±1.0°F overall. Scanner resolution however is more appropriately specified in scanner units rather than actual temperatures, since the conversion from scanner units to temperature (sensitivity) is variable, dependent on atmospheric attenuation, lens configuration, target emissivities, and other parameters. Therefore, the maximum error in scanner units is also presented in Table 8 and is approximately ±0.35 units overall. The relationship between temperature error and scanner error is expressed as

$$E_t = \frac{E_s}{A \cdot S_t} ,$$

where E_t is the error in temperature units, E_s is the basic scanner resolution error, S_t is the scanner temperature sensitivity, and A is the attenuation factor due to atmospheric attenuation, lens configurations, filters, etc. A scanner resolution of ±0.35 units as shown by this analysis is in agreement with general observations of scanner output, particularly in the line scan mode, which shows a noise constant of approximately ±0.25 to ±0.33 units inherent in the instrument.

TABLE 8. TEMPERATURE RESOLUTION TEST RESULTS

TEST 54-0 SENSITIVITY = .344 UNITS/DEGF

TARGET	LEVEL (UNITS)	MEAS TEMP (DEGF)	CALC TEMP (DEGF)	ERROR (DEGF)
ICE	1.0	32.0	32.0	0.0
1	7.5	51.3	50.9	-0.4
2	8.0	52.7	52.4	-0.3
3	8.0	52.7	52.4	-0.3
4	7.8	51.8	51.8	0.0
5	7.4	49.5	50.6	1.1

MAXIMUM SCANNER ERROR =+.378 UNITS

TEST 55-6 SENSITIVITY = .401 UNITS/DEGF

TARGET	LEVEL (UNITS)	MEAS TEMP (DEGF)	CALC TEMP (DEGF)	ERROR (DEGF)
ICE	3.6	32.0	32.0	0.0
1	8.1	42.4	43.2	0.8
2	8.6	44.5	44.5	0.0
3	8.9	45.9	45.2	-0.7
4	9.0	45.3	45.4	0.1
5	8.5	44.4	44.2	-0.2

MAXIMUM SCANNER ERROR =-.321 UNITS

TEST 55-9 SENSITIVITY = .366 UNITS/DEGF

TARGET	LEVEL (UNITS)	MEAS TEMP (DEGF)	CALC TEMP (DEGF)	ERROR (DEGF)
ICE	1.2	32.0	32.0	0.0
1	7.4	49.2	49.0	-0.2
2	8.1	50.6	50.9	0.3
3	8.1	50.8	50.9	0.1
4	7.8	50.0	50.0	0.0
5	7.0	48.0	47.9	-0.1

MAXIMUM SCANNER ERROR =+.110 UNITS

TABLE 8. (Concluded)

TEST 56-2/3 SENSITIVITY = .346 UNITS/DEGF

TARGET	LEVEL (UNITS)	MEAS TEMP (DEGF)	CALC TEMP (DEGF)	ERROR (DEGF)
ICE	0.9	32.0	32.0	0.0
1	-	17.6	-	-
2	3.5	39.5	39.5	0.0
3	7.2	50.6	50.2	-0.4
4	9.0	55.3	55.4	0.1
5	9.4	56.4	56.6	0.2

MAXIMUM SCANNER ERROR =-.138 UNITS

TEST 56-7/8 SENSITIVITY = .318 UNITS/DEGF

TARGET	LEVEL (UNITS)	MEAS TEMP (DEGF)	CALC TEMP (DEGF)	ERROR (DEGF)
ICE	1.9	32.0	32.0	0.0
1	-	18.1	-	-
2	4.6	41.5	40.8	-0.7
3	8.0	51.7	51.5	-0.2
4	9.5	55.9	56.2	0.3
5	9.9	57.0	57.5	0.5

MAXIMUM SCANNER ERROR =-.223 UNITS

TEST 56-9/10 SENSITIVITY = .313 UNITS/DEGF

TARGETS	LEVEL (UNITS)	MEAS TEMP (DEGF)	CALC TEMP (DEGF)	ERROR (DEGF)
ICE	1.7	32.0	32.0	0.0
1	-	17.9	-	-
2	4.2	40.9	40.0	-0.9
3	7.8	51.6	51.4	-0.2
4	9.4	56.0	56.5	0.5
5	9.8	57.3	57.8	0.5

MAXIMUM SCANNER ERROR =-.282 UNITS

5.3 Temperature Sensitivity

As previously discussed, the data output by the IR scanner is in raw scanner units which must be calibrated to obtain actual temperatures. The relationship between scanner units and temperature is the instruments' temperature sensitivity (S_s) expressed in units per °F. This sensitivity is dependent on many factors including the target emissivity, the target temperature (i.e., the sensitivity varies with temperature), atmospheric attenuation, and the scanner optics configuration including lens filters, etc. To determine the sensitivity for given conditions it is required to view two known reference targets under the same conditions. The sensitivity is then calculated as

$$S_t = \frac{I_2 - I_1}{T_2 - T_1} \quad ,$$

where I_1 and I_2 are the scanner readings corresponding to the two reference targets at temperatures T_1 and T_2. Throughout the test program, an ice/water tank and a Freon 114 tank were used as the two reference targets. The thermocouple data from these tanks for the first 17 tests are presented in Table 9. The absolute temperatures shown are in error because the thermocouple reference junction was misadjusted; however, the temperature difference between the tanks is correct. As shown, the temperature difference is fairly stable with an average reading of 6.66°F and a standard deviation of 0.3°F or 4.5 percent.

Possible errors due to the variation of sensitivity with temperature are shown in Figure 12 which depicts the theoretical actual measured temperatures for a scanner calibrated by a 32°F and a 42°F reference target pair. As shown, the error is insignificant within the range of the reference targets and becomes important only at temperatures beyond the range of interest. Therefore, we can neglect sensitivity changes with temperature unless the target temperature is substantially beyond the range of the reference targets.

Using the average temperature difference between the reference tank pair as 6.66°F, the sensitivity was calculated for all the tests with sufficient data available and is tabulated in Table 10. The sensitivity is shown for line scan and isotherm data and the average of the two. For those targets that were not geometrically resolved, a corrected sensitivity was calculated based on the percent resolution for the target and the ambient temperature. It should be realized however that the creditability of the corrected reading is low and is presented for information only.

TABLE 9. REFERENCE TANK TEMPERATURE DATA

Test	Average Ice Temperature	Average Freon Temperature	Delta
1	29.3	36.2	6.9
2	30.0	36.3	6.3
3	30.0	37.0	7.0
4	30.1	36.6	6.5
5	30.4	36.7	6.3
6	30.2	37.1	6.9
7	30.3	37.3	7.0
8	30.5	37.2	6.7
9	30.0	36.7	6.7
10	30.0	36.8	6.8
11	30.1	36.6	6.5
12	29.9	37.0	7.1
13	30.2	37.1	6.9
14	30.3	36.6	6.3
15	30.3	36.8	6.5
16	30.7	36.8	6.1
17	30.3	37.1	6.8
		AVG	6.66
		σ	0.30

Standard lens sensitivities for the 10 scale versus distance are presented in Figure 13. The reference tests were all taken at one distance and show a considerable spread, probably due to viewing angle effects. The multi-distance tests show a slight decrease in sensitivity with distance which was expected (note that the multi-distance data are unresolved after 75 ft).

Figures 14 and 15 present similar data for the 3X telescope lens. The reference test and multi-distance test data are presented in Figure 14, and the resolution and ice/frost test data are presented in Figure 15.

From Figure 14 we see the same decrease in sensitivity with distance as observed with the standard lens. The reference tests which were performed indoors on a rainy day show a lower sensitivity than the multi-distance tests, probably due to the increased humidity. Figure 15

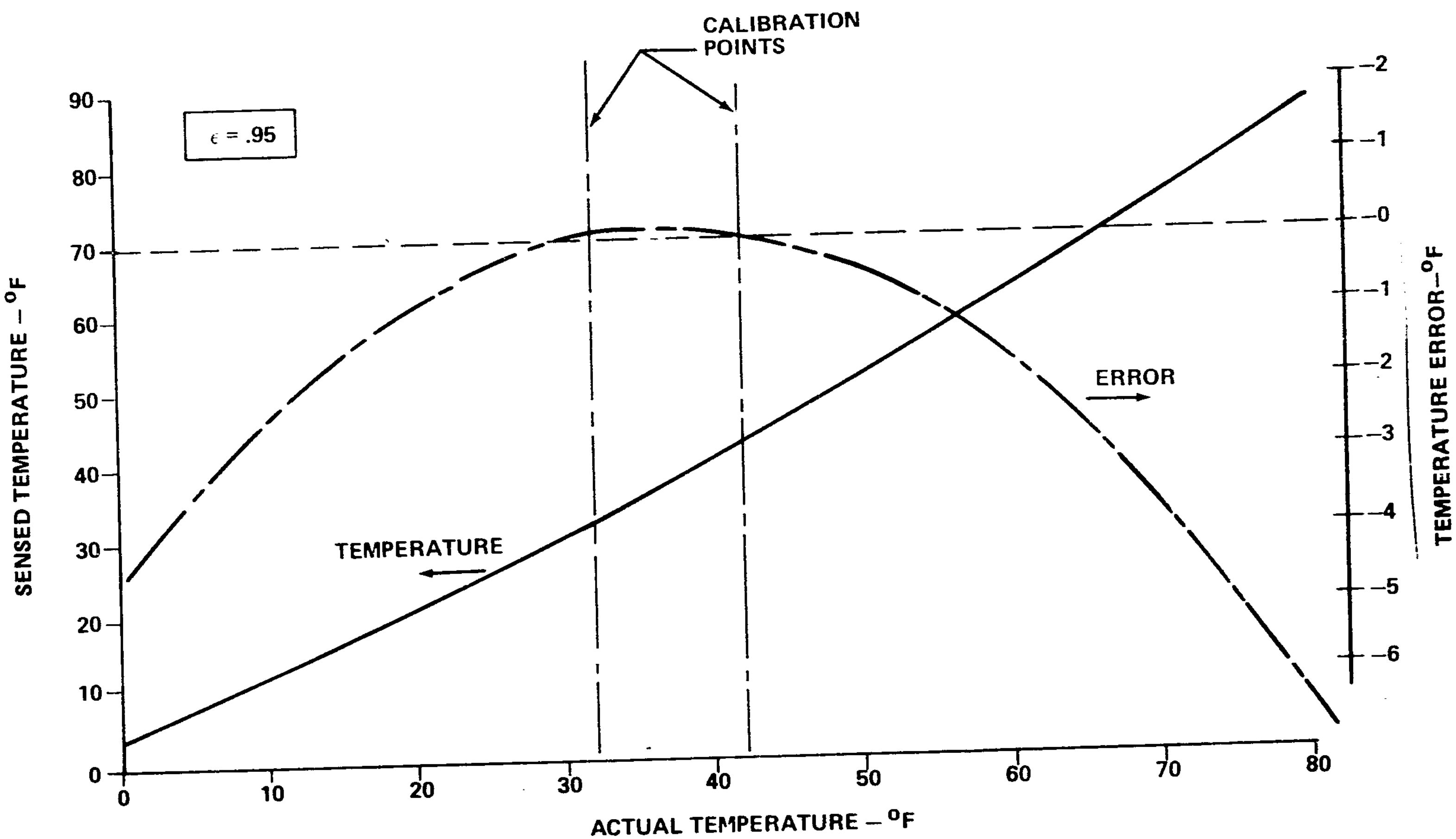

Figure 12. Theoretical scanner error versus temperature.

TABLE 10. IR SCANNER SENSITIVITY DATA

TEST	TYPE	LENS	SCALE	DIST	ANG	RSL	SENSITIVITY LINE SCAN	ISOTHERM	AVERAGE
1	REF	STN	10	25	0	R	.36	.345	.352
2	REF	STN	10	25	0	R	.36	.345	.352
3	REF	STN	10	25	30	R	.3	.315	.307
4	REF	STN	10	25	50	R	.15	.18	.165
5	REF	STN	10	25	50	R	.285	.27	.277
6	REF	STN	10	25	70	R	.3	.21	.255
7	REF	STN	10	25	70	R	.3	.24	.27
8	REF	STN	10	25	70	R	.3	.225	.262
9	REF	STN	10	25	70	R	.285	.27	.277
10	REF	STN	10	25	50	R	.3	.285	.292
11	REF	STN	10	25	30	R	.3	.285	.292
12	REF	STN	10	25	0	R	.285	.27	.277
13	REF	STN	10	25	0	R	.3	.315	.307
14	REF	3X	10	66	0	R	.315	.315	.315
15	REF	3X	10	66	0	R	.315	.285	.3
16	REF	3X	10	100	0	R	.3	.255	.277
17	REF	3X	10	100	0	R	.3	.3	.3
18	FOG	3X	10	75	0	R	.42	.42	.42
19	FOG	3X	10	100	0	R	.3	.375	.337
20	FOG	3X	10	150	0	R	.24	.27	.255
21	FOG	3X	10	200	0	R	.15	.21	.18
22	FOG	3X	10	250	0	U	.15	.225	.187
				CORRECTED			.163	.244	.203
23	FOG	3X	10	300	0	U	.165	.195	.18
				CORRECTED			.189	.224	.206
24	FOG	3X	10	350	0	U	.165	.165	.165
				CORRECTED			.198	.198	.198
25	FOG	3X	10	75	0	R	.375	.465	.42
28	MDIS	STN	10	25	0	R	0	.315	.315
29	MDIS	STN	10	50	0	R	0	.285	.285
30	MDIS	STN	10	75	0	U	0	.27	.27
				CORRECTED			0	.281	.281
31	MDIS	STN	10	100	0	U	0	.255	.255
				CORRECTED			0	.289	.289
32	MDIS	STN	10	150	0	U	0	.24	.24
				CORRECTED			0	.311	.311
33	MDIS	STN	10	200	0	U	0	.21	.21
				CORRECTED			0	.299	.299
34	MDIS	STN	10	25	0	R	.3	.285	.292
35	MDIS	STN	10	50	0	R	.3	.345	.322
36	MDIS	3X	10	50	0	R	.435	.435	.435
37	MDIS	3X	10	75	0	R	0	.42	.42
38	MDIS	3X	10	100	0	R	.45	.45	.45
39	MDIS	3X	10	150	0	R	0	.375	.375
40	MDIS	3X	10	200	0	R	.345	.345	.345
41	MDIS	3X	10	250	0	U	.39	.42	.405
				CORRECTED			.423	.456	.44
42	MDIS	3X	10	350	0	U	.345	.33	.337
				CORRECTED			.41	.392	.401
43	MDIS	3X	10	400	0	U	.375	.375	.375
				CORRECTED			.474	.474	.474
44	MDIS	3X	10	450	0	U	.195	.18	.187
				CORRECTED			.256	.236	.246

TABLE 10. (Continued)

							SENSITIVITY		
TEST	TYPE	LENS	SCALE	DIST	ANG	RSL	LINE SCAN	ISOTHERM	AVERAGE
45	MDIS	3X	10	500	0	U	.315	.27	.292
				CORRECTED			.431	.369	.4
49	SUNR	3X	10	50	0	R	.42	.42	.42
51	SKYB	3X	10	47	30	R	.42	.42	.42
52	SKYB	3X	10	47	30	R	.48	.48	.48
54	T-RES	3X	10	50	0	R	.343	0	.343
55	T-RES	3X	10	50	0	R	.382	0	.382
56	T-RES	3X	10	50	0	R	.325	0	.325
61	G-RES	3X	10	75	0	R	.45	0	.45
62	G-RES	3X	10	300	0	U	.285	.27	.277
				CORRECTED			.327	.31	.318
63	G-RES	3X	10	200	0	R	.42	.405	.412
64	G-RES	3X	10	150	0	R	.39	0	.39
74	ICE	3X	20	75	0	R	.3	.24	.27
75	LDIS	3X	10	800	0	U	.45	.39	.42
				CORRECTED			.529	.458	.494
		2ND TRGT SET		75	0	R	.33	.315	.322
76	DRIZ	3X	10	50	0	R	.36	0	.36
79	LDIS	3X	10	800	0	U	.39	.375	.382
				CORRECTED			.458	.441	.449
		2ND TRGT SET		50	0	R	.36	.36	.36
80	LDIS	3X	10	800	0	U	.375	.345	.36
				CORRECTED			.441	.405	.423
		2ND TRGT SET		50	0	R	.36	.36	.36
84	G-RES	3X	10	30	0	R	.45	0	.45
86	ICE	3X	10	27	0	R	0	.375	.375
90	ICE	3X	10	75	0	R	0	.285	.285
94	ICE	3X	10	75	0	R	0	.33	.33
98	IRR	STN	10	17	0	R	0	.315	.315
99	IRR	STN	20	26	0	R	0	.18	.18
100	IRR	STN	20	26	0	R	0	.15	.15
101	IRR	STN	20	26	0	R	0	.135	.135
102	IRR	STN	20	26	0	R	0	.135	.135
103	IRR	STN	20	26	0	R	0	.15	.15
104	IRR	STN	20	26	0	R	0	.15	.15
105	IRR	STN	20	26	0	R	0	.135	.135
106	IRR	STN	20	26	0	R	0	.135	.135
107	IRR	STN	20	26	0	R	0	.12	.12
108	IRR	STN	20	26	0	R	0	.135	.135
109	IRR	STN	20	26	0	R	0	.15	.15
110	IRR	STN	20	26	0	R	0	.15	.15
111	IRR	STN	20	26	0	U	0	.165	.165
				CORRECTED			0	.175	.175
112	IRR	STN	20	26	0	U	0	.195	.195
				CORRECTED			0	.207	.207
113	IRR	STN	20	26	0	U	0	.225	.225
				CORRECTED			0	.239	.239
114	SUNR	3X	20	33	0	R	0	.255	.255
115	SUNR	3X	20	33	0	R	0	.225	.225
117	IRR	STN	20	32	0	R	0	.09	.09
118	IRR	STN	20	32	0	R	0	.09	.09
119	IRR	STN	20	32	0	R	0	.09	.09
120	IRR	STN	20	32	0	R	0	.075	.075

TABLE 10. (Concluded)

TEST	TYPE	LENS	SCALE	DIST	ANG	RSL	SENSITIVITY LINE SCAN	ISOTHERM	AVERAGE
121	IRR	STN	20	32	0	R	0	.105	.105
123	IRR	STN	20	32	0	R	0	.09	.09
124	IRR	STN	20	32	0	R	0	.105	.105
126	IRR	STN	20	32	0	R	0	.09	.09
127	IRR	STN	20	32	0	R	0	.12	.12
128	IRR	STN	20	32	0	R	0	.105	.105

DIST - Target Distance (ft.)
ANG - Angle to Target Normal (Deg.)
RSL - Resolution R = Resolved, U = Unresolved

Line Scan - Sensitivity from Line Scan Mode (units/^{o}F)
Isotherm - Sensitivity from Isotherm Mode (units/^{o}F)
Average - Average of Line Scan and Isotherm

shows the same distance effects for the geometric resolution tests. The temperature resolution tests and ice/frost tests show a moderate amount of spread probably due to dispersions caused by reference target errors, emissivity shifts, scanner resolution limits, etc.

Figure 16 presents data from the fog tests which used the 3X telescope lens and the 10 scale. As shown there is a significant drop with distance which is substantially greater than would be predicted for atmospheric attenuation under 100 percent humidity conditions. This greater attenuation is attributed to the suspended water particles which are present in fog and effectively increase the atmospheric emissivity.

A summary of the nominal sensitivities for the two lens configurations is presented in Table 11 which is an average of selected data from Table 10. The data selected do not include any tests over 150 ft viewing distance, any tests with unresolved data, or any drizzle or fog tests. These data should be considered as the average sensitivity with the specified deviations for nominal close range viewing conditions.

5.4 Distance Effects

The effect of viewing distance on sensitivity was discussed in the previous section where it was shown that sensitivity decreased with increasing distance. The cause for the decrease in sensitivity is atmospheric attenuation of the target energies coupled with receipt of energy from the atmosphere itself. The predominant parameter affecting atmospheric attenuation is the water vapor content of the atmosphere, since effects from other gases (e.g., CO_2) are insignificant for the

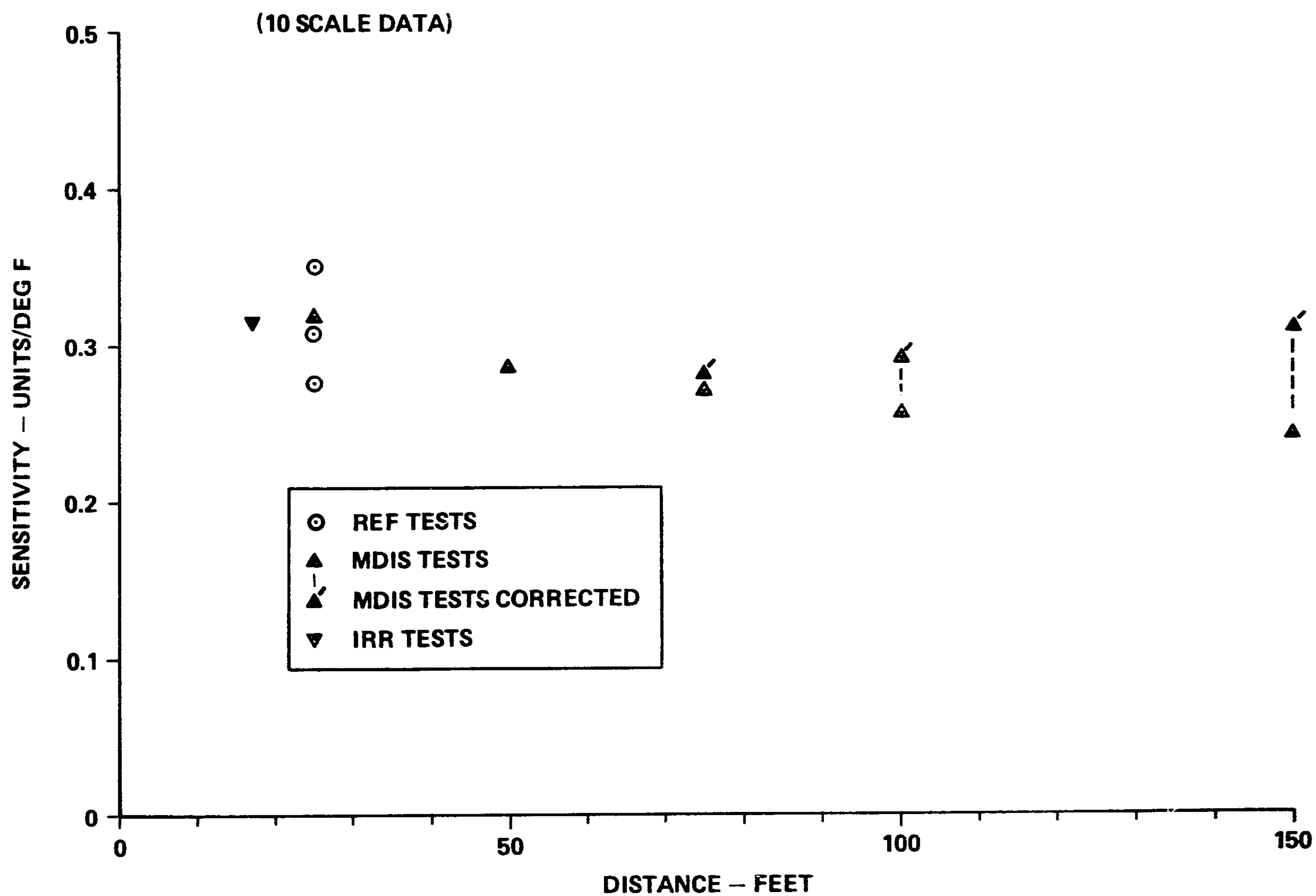

Figure 13. Sensitivity versus distance for the standard lens.

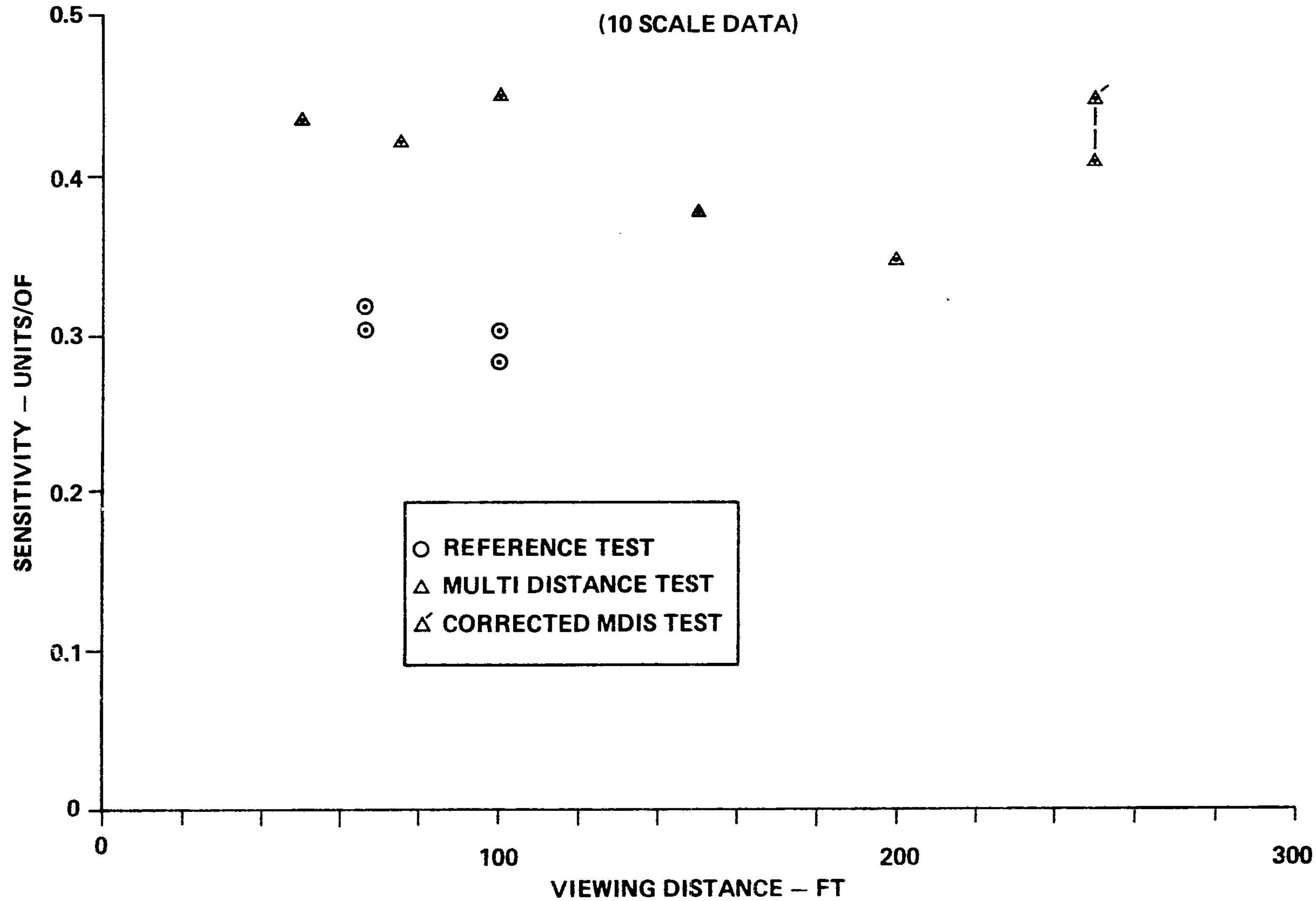

Figure 14. Sensitivity versus distance for 3X telescope lens.

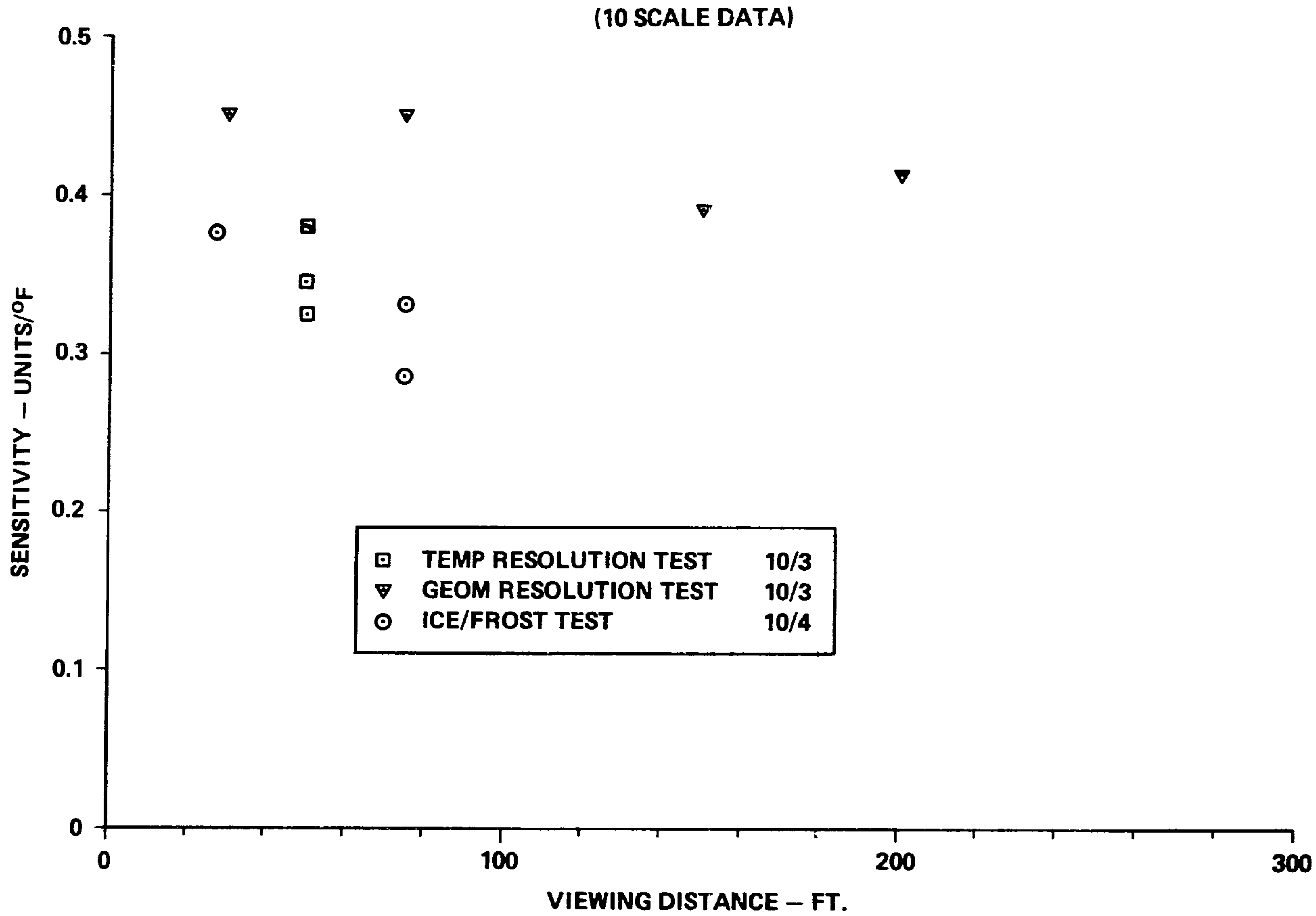

Figure 15. Sensitivity versus distance for 3X telescope lens.

ORIGINAL PAGE IS POOR

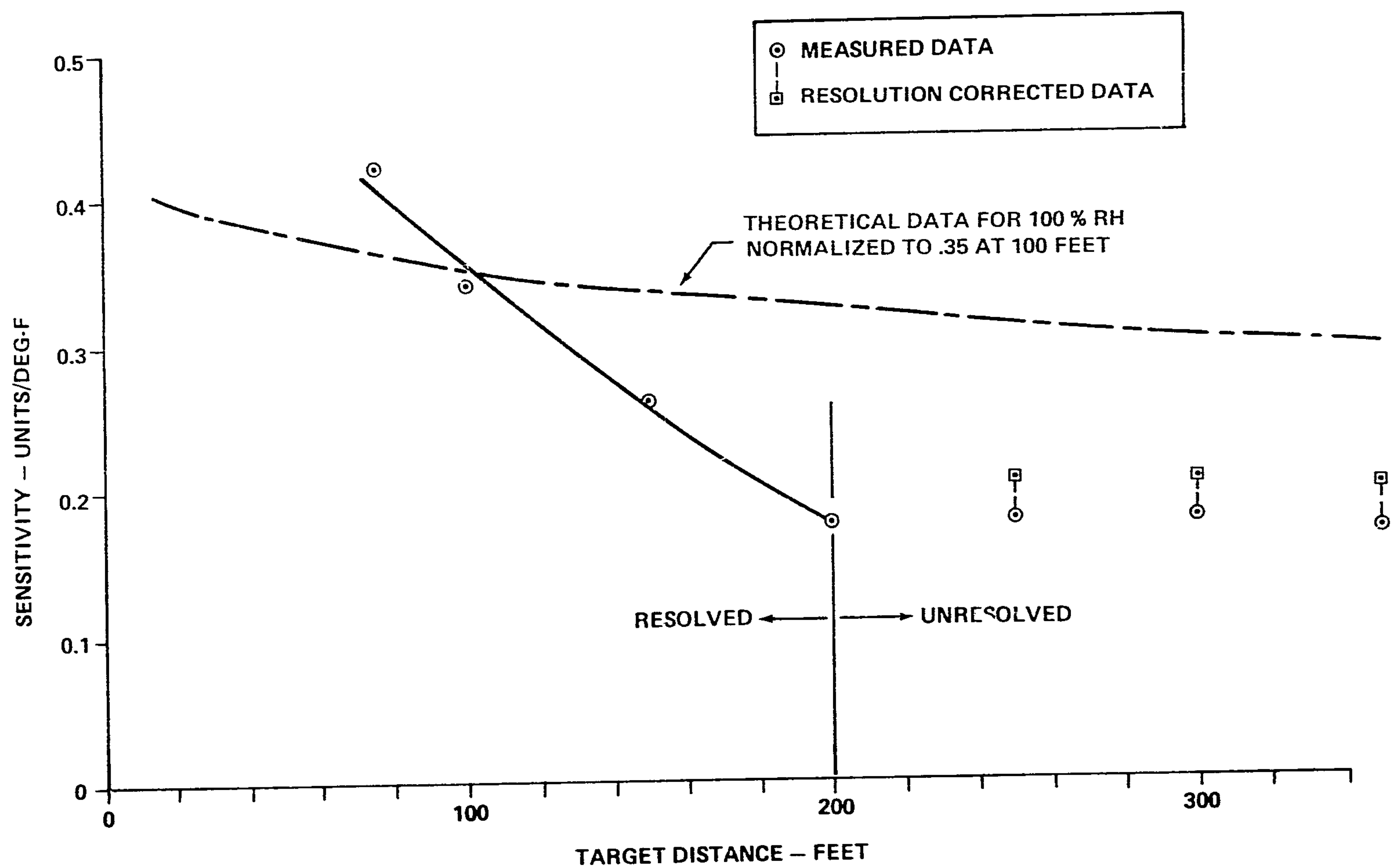

Figure 16. Sensitivity versus distance for fog tests.

TABLE 11. SENSITIVITY AVERAGES

Configuration	Average Sensitivity	Standard Deviation
Standard Lens 10 Scale	0.313	0.0267
Standard Lens 20 Scale	0.144	0.0149
3X Telescope 10 Scale	0.369	0.0618
3X Telescope 20 Scale	0.25	0.0229

bandwidth of the IR scanner (i.e., 8 to 12 microns). The spectral emissivity of water vapor is shown in Figure 17 for two sets of typical conditions. As shown there is a "transmittance window" at the band width of the scanner with the emissivity being insignificant (for the cases shown) between 9 and 12 microns. The stated band width for the scanner (8 to 12 microns) is also shown; however, the vendor has indicated that the cutoff at 8 microns is a gradual roll off such that the scanner is somewhat sensitive to energy above 8 microns. Since this is the edge of the "transmittance window," atmospheric attenuation is highly dependent on the actual bandwidth of the scanner. As indicated in Figure 17 the effective emissivity of the atmosphere increases as the viewing distance is increased or as the water vapor content of the atmosphere is increased (high humidity). In addition to the decrease in scanner sensitivity already noted, the atmospheric attenuation also causes a shift in the apparent target temperature. As the viewing distance is increased, the target temperature appears to approach the ambient temperature, which for the current application would be a temperature increase. This is a potential problem since the viewing distance from a scanner mounted on the Fixed Service Structure (FSS) would vary as the ET is scanned vertically, and for many ET stations would be different than the reference target viewing distance.

The multiple distance tests (reference Section 4.5) were conducted to assess this problem and the resultant data are tabulated in Table 12. The data presented are the apparent temperature shift between two targets at different distances but at the same temperature. Data from the line scan mode and the isotherm mode are included (where available) as well as the average of the two. When both an ice tank pair and a Freon tank pair were used, the overall average of both was computed. As with the sensitivity analysis, corrected data are included for those tests with unresolved targets and are based on the percent resolution and the ambient temperature as follows:

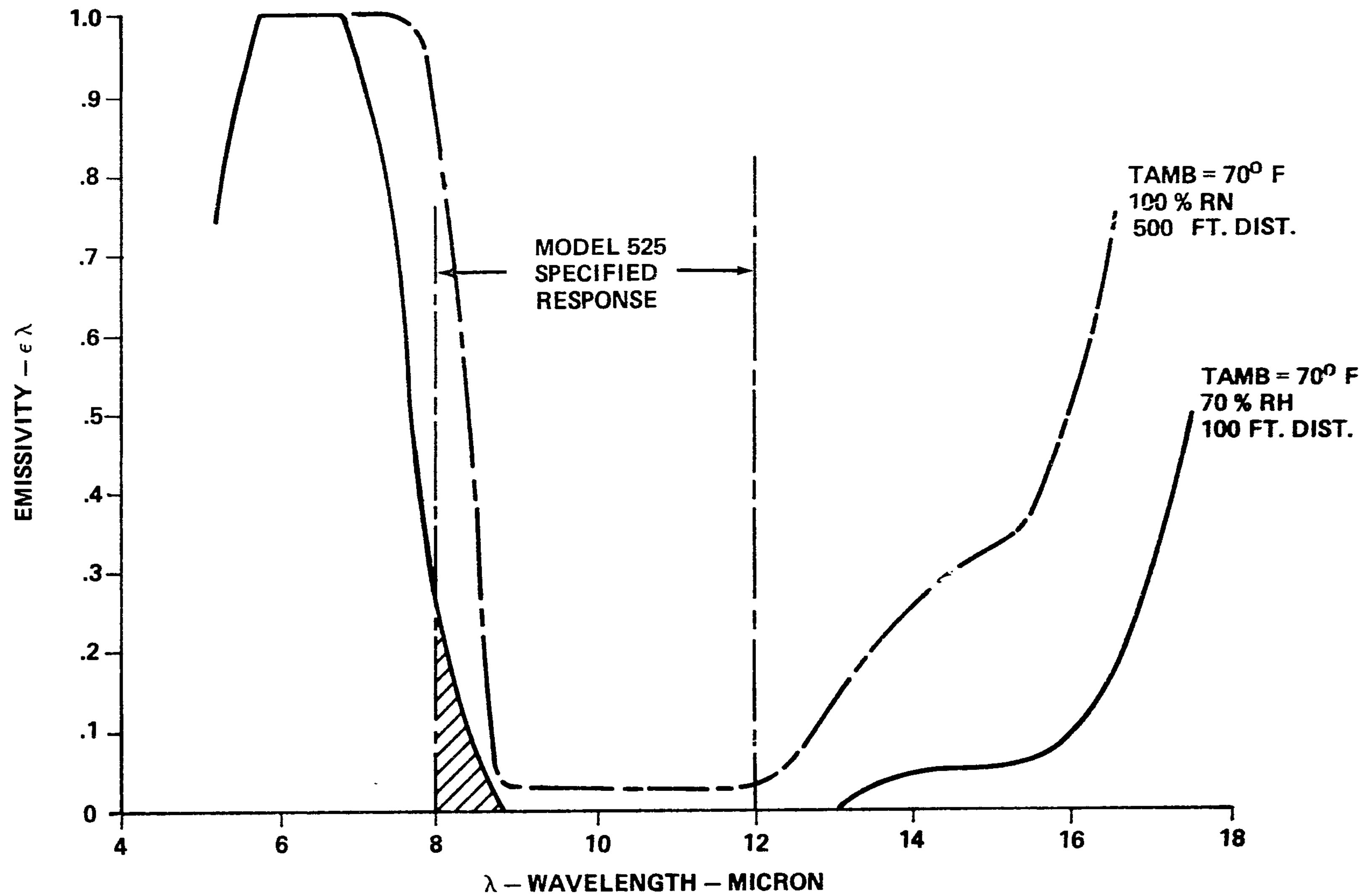

Figure 17. Water vapor emissivity versus wavelength for typical conditions.

TABLE 12. MULTI-DISTANCE APPARENT TEMPERATURE SHIFTS

					ICE1-ICE2			FREON1-FREON2			OVERALL
TEST	TYPE	LENS	DIST1	DIST2	LS	ISO	AVG	LS	ISO	AVG	AVG
28	MDIS	STN	25 R	25 R	0	0	0	0	0	0	0
29	MDIS	STN	50 R	25 R	0	1.3	1.3	0	0	0	1.3
30	MDIS	STN	75 U	25 R	0	3.6	3.6	0	0	0	3.6
			CORRECTED		0	2.1	2.1	0	0	0	2.1
31	MDIS	STN	100 U	25 R	0	7.2	7.2	0	0	0	7.2
			CORRECTED		0	3	3	0	0	0	3
32	MDIS	STN	150 U	25 R	0	11.1	11.1	0	0	0	11.1
			CORRECTED		0	3.1	3.1	0	0	0	3.1
33	MDIS	STN	200 U	25 R	0	14.4	14.4	0	0	0	14.4
			CORRECTED		0	3.5	3.5	0	0	0	3.5
34	MDIS	STN	25 R	25 R	.9	0	.9	0	0	0	.9
35	MDIS	STN	50 R	25 R	1.3	1.8	1.6	0	0	0	1.6
36	MDIS	3X	50 R	50 R	.2	0	.2	0	0	0	.2
37	MDIS	3X	75 R	50 R	0	.2	.2	0	0	0	.2
38	MDIS	3X	100 R	50 R	.6	.9	.8	0	0	0	.8
39	MDIS	3X	150 R	50 R	0	5.1	5.1	0	0	0	5.1
40	MDIS	3X	200 R	50 R	8.1	8.8	8.4	0	0	0	8.4
			CORRECTED		7.4	8.1	7.8	0	0	0	7.8
41	MDIS	3X	250 U	50 R	6.2	5.8	6	0	0	0	6
			CORRECTED		3.2	2.7	3	0	0	0	3
42	MDIS	3X	350 U	50 R	4.8	4.6	4.7	0	0	0	4.7
			CORRECTED		2.1	2.1	2.1	0	0	0	2.1
43	MDIS	3X	400 U	50 R	0	9	9	0	0	0	9
			CORRECTED		0	.3	.3	0	0	0	.3
44	MDIS	3X	450 U	50 R	10.4	11.1	10.8	0	0	0	10.8
			CORRECTED		.4	1.4	.9	0	0	0	.9
45	MDIS	3X	500 U	50 R	8.8	9.5	9.1	0	0	0	9.1
			CORRECTED		3	2.1	2.5	0	0	0	2.5
75	LDIS	3X	800 U	75 R	8.7	8.4	8.6	11.2	9.9	10.6	9.6
			CORRECTED		.8	.7	.8	4.9	3.6	4.2	2.5
79	LDIS	3X	800 U	50 R	7.2	8	7.6	7.7	8.3	8	7.8
			CORRECTED		3.3	4.3	3.8	5.1	5.8	5.5	4.7
80	LDIS	3X	800 U	50 R	7.2	8.3	7.7	7.5	8	7.7	7.7
			CORRECTED		3.2	4.5	3.8	4.7	5.3	5	4.4

DIST1 - Far target distance (ft)

DIST2 - Near target distance (ft)

LS - Line scan data (°F)

ISO - Isotherm data (°F)

AVG - Average of LS and ISO data

$$I_t' = I_a + (I_t - I_a)/f \quad ,$$

where I_a is the ambient scanner level, I_t is the target scanner level, f is the resolution factor (0 to 1), and I_t' is the corrected target scanner level. The target scanner level is then converted to temperature based on the sensitivity from the near targets. As with the sensitivity analysis, the credibility of this corrected data is questionable and is included to help assess trends.

Apparent temperatures versus distance are plotted in Figure 18 for the standard lens, and Figure 19 for the 3X telescope. The data plotted are the apparent temperature of the far target as it is moved away from the near fixed target which is assumed to be at 32°F. Significant errors can result for distance changes as small as 50 ft, particularly at close range. As the viewing distances increase, however, the error due to a delta distance decreases since the function is exponential.

An option available which could be used to reduce multi-distance effects is a spectral filter to sharply cutoff energy above 9 microns, thus eliminating most all of the atmospheric attenuation effects due to water vapor. However, because of the narrower band width the total energy received at the detector is reduced, thus reducing the scanner sensitivity. This in turn results in a higher temperature resolution error (reference Section 5.2). The tradeoff of decreased sensitivity for a significant reduction in distance effects may be desirable and will have to be assessed.

5.5 Reflections

Since most all surfaces, including the ET TPS surface, are not perfect "black body radiators," any determination of surface temperature using IR scanning techniques will involve possible errors due to reflections. Reflectance is the portion of energy incident on a surface which is neither absorbed nor transmitted through the object. Since the transmittance can be assumed zero for the current application, the reflectance can be calculated according to Kirchhoff's law as:

$$\rho_\lambda + \epsilon_\lambda = 1.0 \quad ,$$

where ρ_λ is the reflectance and ϵ_λ is the emissivity of the surface for the spectral band width of interest (i.e., λ = 8 to 12 microns). The emissivity of the current ET white paint (FRL-3) is 0.89 to 0.91 whereas

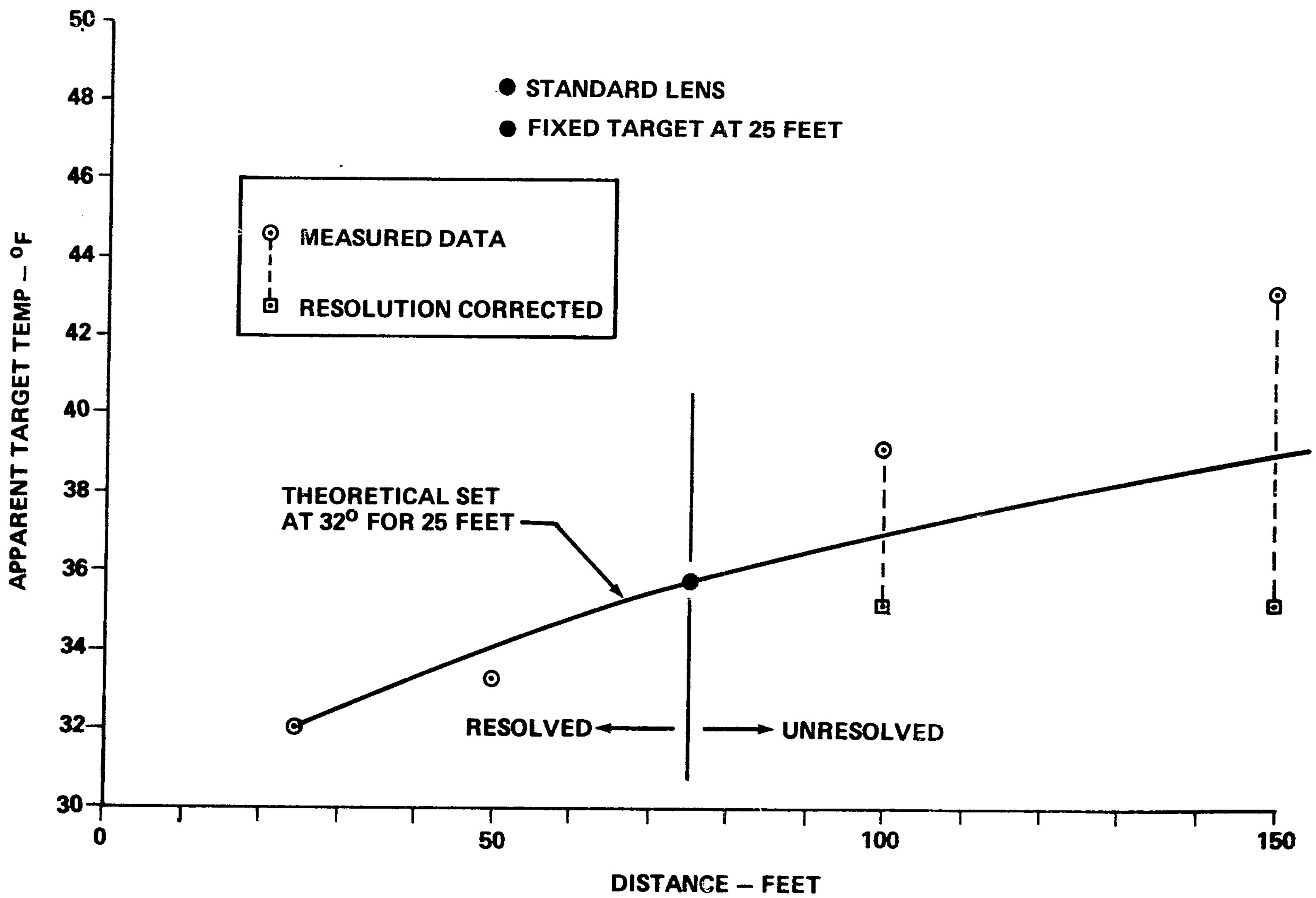

Figure 18. Apparent ice target temperature versus distance.

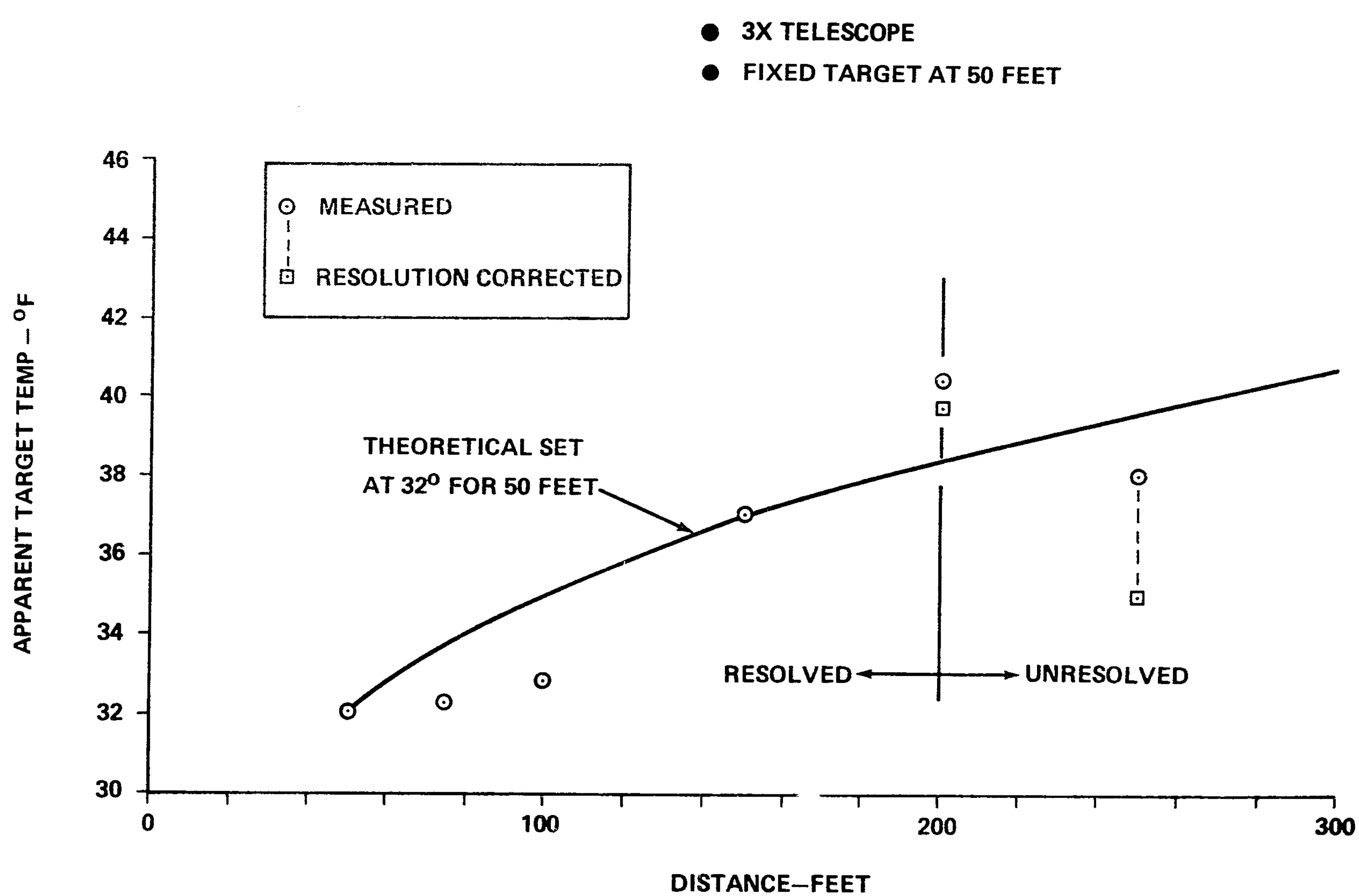

Figure 19. Apparent ice target temperature versus distance.

both water and ice reportedly have emissivities in the 0.94 to 0.96 range. Therefore the reflectance can be expected to be between 0.04 and 0.11 for normal conditions.

For targets with a finite reflectance (i.e., emissivity less than 1), the incoming energy detected by the scanner is the sum of the emitted and reflected energy from the target as follows:

$$E_{sensed} = \varepsilon \times E_{emitted} + (1 - \varepsilon) \times E_{ambient} \quad ,$$

where $E_{emitted}$ is a function of the target temperature and $E_{ambient}$ is dependent on the effective ambient temperature. If the reference targets used to calibrate the scanner have the same emissivity as the target being measured and if the background radiation is the same for both, then the reflected ambient will cancel out in the calibration and there would be no error due to reflections. However, differences in emissivity between the reference and the measured targets, or differing ambient conditions, can cause errors which may become significant. The relationship governing the temperature sensed by a typical scanner, disregarding atmospheric attenuation effects, can be expressed by the following equation:

$$T_s = C_1 + C_2 \left[\varepsilon T_t^4 + (1 - \varepsilon) T_b^4 \right] \quad ,$$

where T_t is the target temperature, T_b is the effective background temperature, and ε is the target emissivity. The above equation can be solved for the various influence coefficients including the target emissivity influence ($\partial T_s / \partial \varepsilon$) and the background temperature influence ($\partial T_s / \partial T_B$). These coefficients are

$$\frac{\partial T_s}{\partial \varepsilon} = \frac{T_t^4 - T_B^4}{4\varepsilon T_t^3}$$

and

$$\frac{\partial T_s}{\partial T_B} = \frac{(1-\varepsilon) T_B^4}{\varepsilon T_t^3}$$

where the appropriate substitutions were made for constants C_1 and C_2. As seen, the target emissivity influence is zero if the target and background temperatures are the same. For background temperatures higher than the target, the influence is negative, and for a background colder than the target, the influence is positive. However, the background temperature influence is always positive. An increase or decrease in the background temperature always causes a corresponding increase or decrease in the sensed temperature. The above equations assume the reference target temperature and the measured target temperatures remain constant. In addition it can be shown that the emissivity influence coefficient is valid for changes in either the reference target emissivity or the measured target emissivity assuming the other is constant. Similarly, the background temperature influence coefficient can be used for changes in effective background temperature at either the reference target or the measured target, assuming the other is unchanged. These influence coefficients have been evaluated for the range of emissivities and background temperatures expected, and are presented in Table 13. Also included in Table 13 are typical temperature errors evaluated for a change in emissivity of 0.05 and a background temperature change of 50°F. As shown, the error due to emissivity shifts within the expected range is approximately ±2.5°F. Errors due to background temperature shifts can be substantial for the lower emissivities, but are generally within ±2.5°F for the higher emissivities of ice and water.

In addition to the normal shift in emissivity between dry and wet (or ice), the emissivity may also vary with viewing angles, particularly at off-normal angles of 45° or more. Published data for water and ice indicate that the emissivity is constant at 0.95 for angles up to 50° where the emittance begins to drop, falling off to below 0.7 for an 80° viewing angle. The IR reflection tests described in Section 4.11 were conducted to assess this problem.

Tests 97 and 98 were conducted in the Building 4561 High Bay area and utilized the large ice reference tank as the target. This target is flat black with an estimated emissivity (normal) of 0.95. During the test, the target was rotated to achieve different viewing angles while maintaining a constant background temperature (i.e., the building). Any change in apparent temperature then should be due to an emissivity shift with angle. Test 97 was conducted with a wet target (condensate) whereas for test 98 the target was wiped dry. As seen in Table 14, both tests exhibited the general trend of reduced emissivities at high viewing angles, with the dry tank showing a higher error than the wet. For viewing angles of 45° or less, the maximum error seen was 1.3°F. However, since only two tests were conducted these data can only be considered preliminary.

To assess other surface coatings, particularly the TPS samples, additional tests were conducted using the surface coating targets listed in Table 2. Since these targets were at ambient temperature, the LN_2

TABLE 13. TARGET INFLUENCE COEFFICIENTS

	T_B = 70°F		T_B = 15°F	
Emissivity	ε = 0.89	ε = 0.96	ε = 0.89	ε = 0.96
$\frac{\partial T_s}{\partial \varepsilon}$	-43.7	-40.5	+48.2	+52.0
Error for $\Delta\varepsilon = 0.05$	-2.2°F	-2.0°F	+2.4°F	+2.6°F
Background Temperature				
$\frac{\partial T_s}{\partial T_B}$	0.152	0.051	0.090	0.030
Error for $\Delta T_B = 50°$	7.6°F	2.6°F	4.5°F	1.5°F

TABLE 14. AMBIENT INFRARED REFLECTION TEST RESULTS

Angle	Level	Level Shift	Temperature Shift	Effective Emissivity
Test 97 Wet 30 × 30 Black Ice Tank				
0	5.7	0	0	0.95 (Assumed)
30	5.7	0	0	0.95
45	5.8	0.1	0.32	0.94
60	5.9	0.2	0.63	0.935
80	6.5	0.8	2.54	0.89
Test 98 Dry 30 × 30 Black Ice Tank				
0	1.8	0	0	0.95 (Assumed)
30	1.8	0	0	0.95
45	2.2	0.4	1.27	0.92
60	2.4	0.6	1.90	0.91
85	5.1	3.3	10.46	0.71
60	2.0	0.2	0.63	0.94
45	1.75	-0.05	-0.16	0.95
30	1.7	-0.1	-0.31	0.95
0	1.7	-0.1	-0.31	0.95

coldplate surface was used as the background to provide a difference in background and target temperatures. The results from these tests are presented in Table 15 which lists the maximum temperature shift seen and the angle. As the targets were rotated toward the LN_2 coldplate surface there was little change noted until the specular angles were reached, where the temperature shift peaked rapidly. This strong specular reflection makes it difficult to assess the data since the temperature shifts shown are due to both background changes and emissivity changes which must be separated to analyze the data. Determination of the background changes involved calculation of the view factor between the sample and the LN_2 coldplate which is complicated by specular reflections. Therefore two sets of emissivity shifts were calculated as the extremes and are presented in Figure 15 with the actual emissivity shift assumed to be within the range shown. Because of the uncertainty in the data, it is difficult to distinguish any difference between the material samples.

TABLE 15. INFRARED REFLECTION FROM LN_2 PANEL TEST RESULTS

TEST	TYPE	LENS	TARGET	NORM TEMP	REFL TEMP	DELTA TEMP	EMISSIVITIES		ANGLE
99	IRR	STN	W-TPS	72	64.9	7.1	.8	.9	52
100	IRR	STN	N-TPS	72	66	5.97	.83	.91	52
101	IRR	STN	W-ALUM	73	68.2	4.84	.86	.93	52
102	IRR	STN	B-ALUM	73	71.1	1.94	.94	.97	51
103	IRR	STN	WB-ALUM	73	70.4	2.58	.93	.96	55
104	IRR	STN	WB-ALUM	73	68.5	4.52	.87	.94	55
105	IRR	STN	W-ALUM	73	68.5	4.52	.87	.94	55
106	IRR	STN	WW-ALUM	75	69.8	5.16	.85	.93	55
107	IRR	STN	W-TPS	75	71.8	3.23	.91	.95	55
108	IRR	STN	WW-TPS	78	73.2	4.84	.87	.93	55
109	IRR	STN	N-TPS	78	71.5	6.45	.82	.91	55
110	IRR	STN	WN-TPS	78	73	5	.86	.93	55
111	IRR	STN	BV-ALUM	78	76.4	1.61	.96	.98	55
112	IRR	STN	WBV-ALUM	78	72.2	5.81	.84	.92	55
113	IRR	STN	BV-ALUM	78	75.1	2.9	.92	.96	55
117	IRR	STN	B-ALUM	75	66.7	8.33	.77	.88	45
118	IRR	STN	WB-ALUM	75	68.7	6.25	.82	.91	45
119	IRR	STN	W-ALUM	75	71.9	3.13	.91	.96	45
120	IRR	STN	WW-ALUM	75	72.9	2.08	.94	.97	45
121	IRR	STN	B-TPS	75	69.8	5.21	.85	.93	45
123	IRR	STN	WB-TPS	75	71.9	3.13	.91	.96	45
124	IRR	STN	N-TPS	75	73.4	1.56	.96	.98	45
126	IRR	STN	WN-TPS	75	73.4	1.56	.96	.98	45
127	IRR	STN	W-TPS	75	72.4	2.6	.93	.96	45
128	IRR	STN	WW-TPS	75	73.2	1.82	.95	.97	45

NORM TEMP - Temperature measured at normal viewing angle.

REFL TEMP - Temperature measured at indicated viewing angle with LN_2 panel reflection.

DELTA TEMP - Difference between NORM and REFL.

EMISSIVITIES - Range of effective emissivities corresponding to REFL TEMP.

However, the black velvet sample (emissivity control paint) did show the least shift of any of the dry samples, and the wet samples generally showed less shift than the corresponding dry samples. An average of all the dry white (FRL-3) samples has a range of 0.88 to 0.94, while an average of the wet white sample is 0.90 to 0.95, slightly higher than the dry.

The averaged wet data which were taken at angles from 45° to 55° (Table 16), compare favorably with the results of the ambient IR test 97 which was also wet, and had a minimum emissivity of 0.935 at 60°. Because of the limited number of tests and difficulty in assessing the data, the results of these tests must be considered preliminary. In addition, since reflections may be the major source of errors, it is recommended that additional tests be conducted to assess this problem.

TABLE 16. INFRARED REFLECTION TEST RESULTS

Sample	Dry Surface Average Range	Wet Surface Average Range
N-TPS	0.87 → 0.93	0.91 → 0.96
W-TPS	0.88 → 0.94	0.91 → 0.95
B-TPS	0.85 → 0.93	0.91 → 0.96
W-ALUM	0.88 → 0.94	0.90 → 0.95
B-ALUM	0.86 → 0.93	0.87 → 0.94
BV-ALUM	0.94 → 0.97	0.84 → 0.92

6.0 CONCLUSIONS

Based on the evaluation of the two IR scanners used in this test program, it can be concluded that the basic scanner capabilities are sufficient to perform the required measurements. However, there are potential problems relating to the targets (i.e., ET) which will require further investigations to properly qualify. The basic concept of using an IR scanner to determine ET surface temperatures, however, does appear feasible.

Performance of the IR scanners used in the test program was generally considered favorable for the intended use. Both geometric and temperature resolutions were adequate and acquisition of data via the various operating modes was satisfactory. The use of a pair of reference tanks for calibration of sensitivity and absolute temperature was successful and is considered practical. No problems associated with vignetting, field of view adjustment (zoom control) or video compatibility were experienced. However, there was noticeable RFI caused by the two-way radios used, which must be considered in the implementation plans.

Generally, the intended targets could be easily acquired (detected) with either ambient or sky backgrounds, at distances up to 800 ft, and in conditions ranging from clear, to drizzle, and fog. The adjustable field of view feature of the Inframetrics Unit (zoom control) was valuable in the acquisition and subsequent evaluation of small targets. The isotherm and the line scan modes were useful in acquiring quantitative data. These data cannot be acquired directly from the scanner since conversion from raw units to temperature must be analytically performed. It is anticipated that for the KSC implementation this function would be performed by a micro- or mini-computer provided within the GSE.

There were no unique problems associated with viewing the simulated ET surface. The rapidly changing surface temperatures experienced with wind and wind simulation did hinder temperature measurements with the scanner although the average temperature could be adequately determined. The use of frame averaging techniques proposed to reduce the system signal-to-noise ratio would also help to lessen wind effects. As expected, the presence of ice or frost on the surface did not present any identifying signature, nor did it interfere with the determination of the surface temperature.

Interference due to solar radiation, either on the targets or incident on the scanner lens, did not present a problem. The same is true for searchlights which have little IR content. However, those lights which have significant IR energy can cause substantial errors.

The most significant problem anticipated concerns the control of the target emissivities and the errors associated with IR reflections. Any change in target emissivity and/or background radiation results in errors in the sensed surface temperature which may become significant. Emissivity which normally varies due to surface contamination and paint variations can also change due to water (condensate) accumulation, and most significantly due to off-normal viewing angles. It is anticipated that a viewing angle constraint (e.g., ±45°) will be imposed to control this problem which will result in some areas of the tank being unobservable. Also selection of reference tank locations must consider background radiation on the reference tank as compared to the ET as well as any viewing angle constraints. It is recommended that additional tests be conducted to assess emissivity changes and associated reflection errors. These tests should further characterize the surface coating which is currently on the ET as well as any alternate coatings or paints which may be more desirable.

Based on the data obtained in this test program together with estimates of unknown or preliminary data, an overall error assessment of the planned scanner/target system can be made. Table 17 is a summary

TABLE 17. BASIC SCANNER TEMPERATURE RESOLUTION

A. Scanner Resolution As Tested	E_s = ±0.35 Units
B. Scanner Resolution With Enhancements	E_s = ±0.20 Units (estimated)
C. Scanner Sensitivity	S_t = 0.29 Units/°F (worst case) = 0.43 Units/°F (best case)
D. Attenuation Factor	A = 0.7 (worst case) = 1.0 (best case)
E. Basic Scanner Temperature Resolution $(E_t = \frac{E_s}{A \times S_t})$	E_t = ±1.72°F (worst case) E_t = ±0.99°F (worst case enhanced) E_t = ±0.47°F (best case enhanced)

of the scanner capabilities and the resulting basic scanner temperature resolution. Item A is the scanner resolution (in scanner units) as determined from the current test data, and item B is the estimated scanner resolution with various signal processing enhancements which are currently available. These enhancements include an optional 8-bit processor within the scanner which increases the scanner's resolution (6-bit processor is standard) and a video frame averager which would increase the signal-to-noise ratio, effectively increasing the sensitivity. Using the range of scanner sensitivities (item C) and attenuation factors, representing atmospheric effects, possible filters, or both (item D), the temperature resolution can be calculated as in item E. As seen, the worst-case resolution without enhancements is ±1.72°F. With the mentioned enhancements, the resolution should improve to ±0.99°F; considering both the enhancements and the best case parameters, the resolution would be ±0.47°F. These limits represent the basic accuracy of the instrument and do not account for additional errors due to adverse viewing conditions or due to target emissivity uncertainties. Table 18 presents the overall error assessment for the combined scanner-target system. Item A is the basic scanner accuracy (enhanced) previously discussed and is the smallest contributor. Item B is the uncertainty in the measured reference target temperature. With proper signal conditioning and calibration, it is estimated that accuracy of at least ±1.0°F can be achieved and hopefully ±0.5°F. Item C represents multiple distance effects, between the reference target and the ET, which cannot be corrected either analytically or with filters. Item D is the error caused by uncertainties or changes in the target emissivities including viewing angle variations. The worst-case figure allows for an emissivity change of 0.07, whereas the best-case figure represents a 0.04 change.

TABLE 18. OVERALL ERROR ASSESSMENT

	Worst Case	Best Case
A. Basic Scanner Temperature Resolution	±0.99	±0.47
B. Reference Target Uncertainty	±1.0	±0.50
C. Uncorrectable Multi-Distance Effects	±1.5	±0.50
D. Emissivity* Variation	±3.0	±2.0
E. Background* Variations	±3.0	±1.0
RSS	±4.7	±2.4

*Note: These are design goals.

Finally, item E is the error caused by background temperature variations between the reference target and the ET and represents a 50°F shift for the worst case and a 20°F shift for the best. In both cases, an influence coefficient of 0.05 was used which is for high emissivities (reference Table 13). Items D and E are design goals which may require certain design and/or operational constraints to meet (e.g., viewing angle limits), and in addition are based on the preliminary data contained herein. As such these items are the least certain at this time. The resultant RSS error for the worst case is ±4.7°F and ±2.4°F for the best case. Although errors of this magnitude are undesirable, they are considered to be within the requirements for the intended use.

It is recommended that additional testing be conducted in the area of emissivity variations, and IR reflections in general, to further assess and possibly reduce these errors.

APPROVAL

INFRARED SCANNER CONCEPT VERIFICATION TEST REPORT

By F. D. Bachtel

The information in this report has been reviewed for technical content. Review of any information concerning Department of Defense or nuclear energy activities or programs has been made by the MSFC Security Classification Officer. This report, in its entirety, has been determined to be unclassified.

J. L. Vaniman

J. L. VANIMAN
Chief, Thermal Engineering Branch

J. B. Sterett

J. B. STERETT
Acting Chief,
Engineering Analysis Division

A. McCool

A. A. McCOOL
Director
Structures and Propulsion Laboratory